

Dear Editor,

Herewith we submit the revised manuscript acp-2016-436, “Data assimilation for volcanic ash plumes using a Satellite Observational Operator: a case study on the 2010 Eyjafjalla­jökull volcanic eruption”. First we would like to thank you and the three anonymous reviewers, and really appreciate the detailed comments and suggestions. We have carefully considered all the concerns and made changes accordingly in the revised paper. We believe the new version has been improved a lot compared to the previous version. In the new version, with the agreement of all authors, we have changed the author’s order to Guangliang Fu, Fred Prata, Hai Xiang Lin, Arnold Heemink, Arjo Segers, Sha Lu.

In the following we will give our answers and reactions to the comments. To make the changes easier to identify, we have numbered them.

Best regards,  
Guangliang Fu  
on behalf all co-authors

(The revised manuscript is **in the latter part of this pdf.**, Changes for Reviewer#1: “blue”; Reviewer#3: “red”; Reviewer#4: “purple”)

# Reply to Reviewer #1:

## Specific comments:

1. *As already pointed out in my former review, the authors discuss the situation that there is an ash layer in clear-sky atmosphere. However, in general there are water and ice clouds above/below/within the ash layer, and situations where clouds move above the ash layer. In such situations the ash layer can't be detected by the satellite algorithms (e.g., Prata and Prata, 2012), leading to wrong assimilation input. I expect that in such cases the model run without assimilation will perform much better than the assimilated one. I suggest to (1) add a comment on that in the paper, and (2) discuss how these errors are treated in your equation (8).*

### Response:

Yes, this is a good point. We have added a comment and a discussion on this issue in [line\(s\) 7.6–7.12](#):

“ Note that in this study we discuss the situation that there is an ash plume in clear-sky atmosphere. However, in general there are water and ice clouds above/below/within the ash plume, and situations where clouds move above the ash layer. In such situations the ash plume cannot be detected by the satellite algorithms (Prata and Prata, 2012), leading to wrong assimilation input. For these reasons the SEVIRI retrieval takes a very conservative approach with lots of different thresholds and conditions to be met before a pixel is deemed to be ash-affected. Thus the error is more likely to be towards under-estimating the amount of ash. There is an error associated with the ash retrieval that reflects the confidence of the detection algorithm, as well as the error estimates on the derived quantities. Therefore under these situations, the SOO errors are also more likely to be an under-estimation. ”

2. *P 2, L 19: Reference to Lu et al., 2016a is not an adequate reference dealing with satellite observations and does not bring added value to the manuscript. But my main criticism is that it is not a good practice to insert unrequested references to own papers during the review process, even without highlighting the change in the “track change” document. See also [http://www.atmospheric-chemistry-and-physics.net/about/publication\\_ethics.html](http://www.atmospheric-chemistry-and-physics.net/about/publication_ethics.html).*

### Response:

Agree. It is removed in [line\(s\) 2.23](#):

“ satellite observations (Stohl et al., 2011; Prata and Prata, 2012), ”

3. *P 3, L 9 – L19: I really appreciate this nice overview on the vertical extensions of ash layers reported in literature.*

### Response:

Thanks.

4. P 3, L 20 – 22: *The sentence “Thin ash clouds, by their nature are of less concern to aviation because such clouds would be traversed rapidly avoiding the possibility of particle build-up that might lead to engine failure.” is problematic as vertically thin layers are not necessarily traversed rapidly in the horizontal direction. Although the statement might be true in many cases it is not difficult to construct a (realistic) scenario where it is not true. Also, “avoiding” is a rather strong word here. I suggest to use “reducing” or “minimizing” in this context.*
5. P 3, L 20– 22: *“From a modeling perspective lack of vertical resolution in model wind data makes it not useful to make the cloud depth any less than 500 m.”: I don’t think that this argument is conclusive here. The transformation from 2D satellite data to 3D fields is done prior any con- tact with the model wind fields; as you state “The outcome of SOO can be considered as preprocessing to the satellite data assimilation system.”*
6. P 3, L 20 – 22: *To me it still remains a shortcoming that the authors do not consider the full range of observed vertical thickness, 100 m – 3 km. Although I now agree that the vast majority is within the considered range, there is no scientific reason to restrict the analysis on these cases. (In the vast majority of days there is no volcanic ash in the European airspace but nobody would argue that this is a adequate reason to not consider such rare events...)*

Response:

The comment 4 is a good point. Moreover, “avoiding” has been changed to “reducing”. We also agree with both the comment 5 and comment 6. We have re-written this part based on these three very useful comments. We employ 0.2–3.0 km as the most reasonable range (based on literature) for the Eyjafjallajökull volcanic plume, and we re-run experiments based on the new considered range. We also add a note for the 2006 Chaiten eruption, the thickness range of 0.1–0.4 km should be better recommended. All of this part is re-written in [line\(s\) 3.29–4.5](#):

“ For the vertical thickness information of volcanic ash clouds, Schumann et al. (2011) investigated on the 2010 Eyjafjallajökull eruption using airborne data that the volcanic ash clouds spread over large parts of Central Europe, mostly from hundreds of meters to 3 km depth. This is consistent with the results of (Marenco et al., 2011) who observed layer depths between 0.5 and 3.0 km. Dacre et al. (2015) also examined the ground-based lidar data for the Eyjafjallajökull eruption and found a mean layer depth of  $1.2\pm 0.9$  km and compared this with model based estimates of  $1.1\pm 0.8$  km. Prata and Prata (2012) found variable thicknesses ranging from 0.2 up to 3 km. The vast majority of data suggest thickness in the range 0.2–3 km for the 2010 Eyjafjallajökull eruption. Based on these investigations, it is not realistic to use a deterministic value to represent the overall ash cloud thickness, but we can reasonably assume that the thickness has a range of 0.2–3.0 km at the corresponding horizontal location of the SEVIRI retrieved measurements. Although this thickness information is not deterministic, its uncertainty spread is suitable in an observational operator for satellite data assimilation. Note that the thickness range can be different for other volcanic eruptions. For example, Prata et al. (2015) reported low cloud thickness with 80% of cases for the 2006 Chaiten eruption less than 400 m, thus a thickness range of 0.1–0.4 km is recommended for that eruption. ”

7. P 5, L 8 – 9: *“lowest possible thickness” should be “lowest expected thickness” or “lowest considered thickness”*

Response:

Thanks. It is changed to “lowest considered thickness” in [line\(s\) 6.6–6.7](#):

“ The blue layer in [Fig. 2](#) is determined by the lowest considered thickness ”

8. *P 6, L 8 – 9: Figure 1c does only report errors of ash load for pixels where volcanic ash is detected. What is about the error of pixels where no ash is detected? There might be ash as well (for example ash concentration below the detection threshold or ash which is hidden by meteorological clouds). I think the latter should also go into the  $ML_{error}$  ?*

Response:

Yes I agree. The SEVIRI product includes a confidence level that indicates how well/badly the “detection” (not the retrieval) has performed. As a confidence value it is difficult to include in a quantifiable manner into the scheme. There is a discussion of this in Kristiansen et al. (2015) but we admit this is a shortcoming.

9. *P 8, L 22: It is not an objective argumentation to select a small area of the whole region (like Netherlands here), where good agreement is achieved, and to discuss the numbers in a way (observations 3.1 mg/m<sup>2</sup> versus EnSR values of 2.9 - 3.2 mg/m<sup>2</sup> ) implicetely suggesting that the assimilation performance is that close to observations in general. This suggestion even supported by using “for example” in L 22. However, the Netherlands are one of very few areas where you achieve that good agreement. There are even regions with similiar size like the Netherlands, namely the fjord area of Norway or the area around Norfolk/Suffolk in England where the non-assimilated run is much closer to observation than the assimilated run. These findings should be reported in a fair and objective way as well*

Response:

Yes, this is a good point. Also combined with another Reviewer’s comment, we have rewritten the related parts (note that due to we use the thickness range of 0.2–3 km, thus the assimilation result is not exactly same with previous version and we evaluate the new plot by considering the reviewer’s concern) in [line\(s\) 9.22–9.27](#):

“ During two-days continuously assimilating SEVIRI measurements of the extracted PM<sub>10</sub> concentrations, without loss of generality, the analyzed volcanic ash state at 12:00 UTC 17 May/ 00:00 UTC 18 May 2010 is shown in [Fig. 5c/ Fig. 6c](#). The conventional simulation without assimilation is also presented ([Fig. 5b/ Fig. 6b](#)), which is currently the commonly used strategy for the simulation of volcanic ash transport (Webley et al., 2012; Fu et al., 2015). It is clear that in almost the entire plume, the mass loadings by EnSR with SOO are in a better agreement with the SEVIRI mass loadings. It can be seen that EnSR with SOO effectively decreases the estimation level compared to the conventional simulation.

and also in [line\(s\) 9.30–9.33](#):

It should also be noted that while the assimilation does correct a rather large bias in the pure model output, it doesn’t mean that the DA result is better in all locations. For example, in locations around Iceland, the DA doesn’t lead the pure model; At a location (-1°W, 58°N) around England (see [Fig. 5a](#)), the simulation without assimilation seems to match better. ”

10. *P 9, L 15 – 25: The aircraft measurements represent  $PM_{10}$  concentration at inlet position  $(x,y,z,t)$  while the model gives values which are averages of the concentration for a  $0.25^\circ \times 0.1^\circ \times 1$  km grid box. Please justify why is it appropriate to compare these two values.*

Response:

Thanks. I have to say that is the best we can do given that the measurements are made at different resolutions and by different methods. We have added a note related to it. in [line\(s\) 15.15–15.18](#):

“ Note that the aircraft measurements represent  $PM_{10}$  concentration at inlet position while the model gives values which are averages of the concentration for a  $0.25^\circ \times 0.125^\circ \times 1$  km grid box. Assuming the uniformity of the fields, it is appropriate to compare these two values given that the measurements are made at different resolutions and by different methods. However, when the heterogeneity is a serious issue, the model representation error should also be better considered. ”

11. *Figure 1: While there is a continous colour scale in Fig. 6b, there are only five colors in the figure. Is the top height retrieval discrete in a way that it turns out only discrete values of 4, 5, 6, 7, and 8 km? I don't think so, as the KNMI height product documentation shows continous values of top heigts.*
12. *Figure 1: This is true for Fig 1a-c, but also several other figures in the manuscript: While zooming into the pdf file it seems that your plot consists of (intransparent) overlapping colored dots which is not the state of art how to plot a 2D satellite retrieval. I.e., the final figure depends on the sequence of the underlying data. I suggest to revise these figures.*

Response:

Thanks for the comment 11 and 12 in plotting. The dot plot is because the SEVIRI does not sample contiguously. I agree the previous plotting contains overlapping colored dots. In the new version, as suggested, we have re-plotted all the SEVIRI-related figures.

13. *Figure 6: The measurement values plotted in Fig. 6b are not consistent with the (same) measurement data reported in Weber et al., 2010, see <http://dx.doi.org/10.1016/j.atmosenv.2011.10.030>. For example, at 10:00 UTC Weber et al., 2010 reports on  $PM_{10}$  concentration values slightly below/above  $200 \mu\text{g}/\text{m}^3$  whereas Fig 6b indicates values at 10:00 UTC of  $130 \mu\text{g}/\text{m}^3$  which is a approx. 35% smaller value. This is important here, as this incostistency pimps the general agreement of aircraft measurements and EnSR result in the figure.*
14. *Figure 6: Same is true for Fig 6c where Weber et al. 2010, Fig. 8 report on values of approx.  $300 \mu\text{g}/\text{m}^3$  at 13:05 UTC while the authors data report values of  $200 \mu\text{g}/\text{m}^3$ . Please clarify.*

Response:

This is a good point. We upload the original aircraft data (see Supplement), from which the exact value at 10:00 is  $168.4 \mu\text{g m}^{-3}$ . The original continuous values are sampled every 6 seconds. In our previous plotting, we plotted the continuous concentrations every 1 minute, thus we averaged 10 values. In that way, the continuous plot would be smoother and thus easier for comparison. The same clarification is for 13:05 that the original value is  $220.3$

$\mu\text{g m}^{-3}$ . In the new version, to be consistent with the original data, we have re-plotted the continuous values.

**Minor comments:**

1. *P 4, L 17: “caled” should be “called”*

Response:

Corrected in **line(s) 5.6**.

2. *P 7, L 4: broken sentence structure.*

Response:

Revised in **line(s) 8.10–8.11**:

“ The stochastic Plume Height (PH) is assumed to be temporally correlated with exponential decay. The correlation parameter  $\tau$  is set to be 1 hour (Fu et al., 2015). ”

3. *P 8, L 8 + L 9: comma seem to be misplaced.*

Response:

Thanks. Corrected in **line(s) 9.10–9.13**:

“ Note that, in this study only  $\text{PM}_{10}$  ash component is considered in the assimilation system. This is consistent with that (during satellite retrievals) only the fine particles (mostly with sizes  $<10.0 \mu\text{m}$ ) can be detected in the tropospheric volcanic plume based on the robust and reliable retrieval algorithms (Prata, 1989; Corradini et al., 2008). ”

# Reply to Reviewer #3:

## Comments on Section 3.1:

### 1. Comments on Section 3.1:

(1) *I have not understood the concept of the procedure. Maybe other readers will have similar problems, remember that this topic was also raised by the reviewers of the first submission of the manuscript. I don't state that the approach is wrong, but the description is confusing and obviously not all required information are given: In particular it is not clear, what is prescribed/fixed and what is variable. So I encourage the authors to rephrase this section in such a way that nothing remains unclear or might be misunderstood, with text/equations/figure being consistent. Expressions as "extraction layer" can hardly be associated to an atmospheric feature, so a more intuitive name should be chosen to facilitate the understanding. Clarity of this section is essential as it is one of the most important parts of the paper and covers the novelty of the study.*

### Response:

Thank you very much for very helpful comments and explain to us the possible confusion in every step. We have fully re-written this part according to the details questions. We first answer your questions one by one. First, I agree that "extraction layer" is not a good name, we have changed it to "target layers" in [line\(s\) 6.6–6.7](#):

“ [the target layers used in this study refer to both blue and yellow layers.](#) ”

(2) *The following remarks/comments/attempts of interpretation may illustrate my confusion:*

*From SEVIRI mass loading is derived. This is converted to the vertical column by a simple (but sufficiently accurate) approach using Eq. (1). Thus, the remark on page 2/line 35 ('the path can be a line or a curve...') can be omitted, especially as it is more confusing than explaining.*

### Response:

Agree. Omitted as suggested.

(3) *The second parameter derived from SEVIRI is  $H_{top}$ . Here, a typical accuracy of this value should be given. Then it is stated that "the thickness of the plume is investigated". What does this mean? "Investigated" implies that the thickness is varied and a specific/best value is selected by a clearly defined independent criterion. However, neither a definition and an explanation is given.  $T_{low}$  and  $T_{high}$ , and the incremental thickness  $T$  are prescribed. Thus, all other values ( $T_i$ ,  $C_i$ ) are also fixed and depend on the measured  $ML_{vert}$  in the same way in all cases.  $C_i$  does not depend on  $H_{top}$ ; that indeed can to be understood.*

### Response:

Here, "Investigated" is not a suitable word. We choose a reasonable assumption on the thickness range based on a literature review in introduction. Now we re-written this sentence in [line\(s\) 6.3–6.4](#):

“ As introduced in Section 2, the cloud top height ( $H_{\text{top}}$ ) is available from satellite remote sensing and the appropriate thickness range (from  $T_{\text{low}}$  to  $T_{\text{high}}$ , i.e., 0.2 to 3 km) of the plume has been chosen for this case based on a literature review. ”

(4) What is the reason to use different symbols ( $H$  and  $T$ ) for lengths, and not similar symbols for similar quantities; especially  $T$  should obviously be something like  $\delta H$ . The current nomenclature leads to unnecessary confusion. The same is true for  $ML_{\text{vert}}$ . This should be  $M_{\text{vert}}$  or  $m_{\text{vert}}$ , two characters for one quantity are not common in physics, especially as part of equations (it cannot be distinguished from a product of  $M$  and  $L_{\text{vert}}$ )! By the way: to be consistent with a range of possible thicknesses between 0.5 km and 3.0 km,  $N_s$  should be 51, not 50.

Response:

We agree all suggested changes, but would prefer to keep  $H$  and  $T$  different, since  $H$  means Height and  $T$  means Thickness for different things.  $ML_{\text{vert}}$  has changed to  $M_{\text{v}}$ . In this version, we have re-considered a more suitable thickness range of 0.2–3.0 km, thus now  $N_s$  is corrected to 57, not 56 as previous one. This part is in line(s) 6.8–6.16:

“ The details are formulated as follows. First we define

$$N_s = \left\lceil \frac{T_{\text{high}} - T_{\text{low}}}{\Delta T} \right\rceil + 1 \quad , \quad (2)$$

$$T_i = T_{\text{low}} + (i - 1) \times \Delta T, \quad C_i = \frac{M_{\text{v}}}{T_i}, \quad i = 1, 2, \dots, N_s \quad , \quad (3)$$

where  $\Delta T$  is a step length and  $N_s$  is the number of the possible thickness.  $T_{\text{low}}$  represents the blue layer (see Fig. 2) with the fixed thickness of 0.2 km and  $T_{\text{high}} - T_{\text{low}}$  (i.e., the subtraction between  $T_{\text{high}}$  and  $T_{\text{low}}$ ) represents the yellow layer with the fixed thickness of 2.8 km.  $\Delta T$  is chosen at a small value compared to  $T_{\text{low}}$ , which guarantees  $N_s$  is not too small (e.g., less than 2) to have a sufficient number of sample thickness  $T_1, T_2, \dots, T_{N_s}$ . (e.g.,  $\Delta T$  is chosen as 0.05 km in this case study, thus  $N_s$  is calculated as 57.) ”

(5) Eq.(4) assumes that each thickness (0.5 km, 0.55 km, 0.6 km, ..., 2.95 km) has the same probability (cf. line 18 on page 5): is this meant by the authors? Is a consequence of this that the vertical distribution (expressed as  $C_i$ ) is unchanged during the dispersion of the ash-cloud? A variable thickness of the ash-layer (i.e. realistic conditions) is only possible, if  $T_{\text{high}}$  (i.e.  $N_s$ ) is changed. Is this indicated by the authors' remark “Corresponding to the sampled thickness...”? However, it remains open what “the sampled thickness” is and how it is derived.

Response:

Yes, what you understood is what we meant. The sampled thickness is  $T_i$  and it is derived based on Eq. (3). We have clearly stated it as in line(s) 6.17–6.18:

“ Corresponding to the sampled thickness (i.e.,  $T_1, T_2, \dots$ ), the ash concentration can be calculated also as a sample from  $C_1$  to  $C_{N_s}$  through Eq. (3). ”

(6) The paragraph starting at line 27 (page 5) is also difficult to understand. How can it be inferred from Eq. (3) that the concentration in the “yellow region” is zero? Where is an information like “the cloud thickness is 1 km” derived from? It seems contradictorily if



*the thickness is stated to be 1 km, but the ash concentration is allocated to a 0.5 km layer (“between 7.5 km and 8.0 km”). Fig. 2 suggests that the ash layer is always  $T_{top}=0.5$  km thick.*

Response:

This part is redundant and easily confuse the readers. In the new version, our target layers are extended to both blue and yellow layers. We have removed this paragraph to avoid the misleading information.

*(7) If parts of the procedure are only used to estimate the “extraction error”, it should be clearly stated here.*

Response:

Thanks. We have moved the information to the following “SOO error” part.

*(8) I hope that a revision of this section is possible to get a convincing description of the methodology! Maybe it is sufficient to add two “carefully formulated” sentences, especially on the selection/derivation of the “thickness of the ash layer”, and all problems are solved.*

Response:

Thanks for all the discussions above. Benefitting from them, the full Section 3.1 is re-written in line(s) 5.24–6.23:

“ The derivation of the Satellite Observational Operator (SOO) is shown in Fig. 2. The retrieved values by SEVIRI for the ash mass loadings ( $M$ ) can be taken as an integration of ash concentrations along the retrieval path. In principle, the satellite retrieval path could be complicated but generally it is assumed to be a straight line (along the line-of-sight, ignoring refraction) from the measuring apparatus. The angle between the local zenith and the line of sight to the satellite is called Viewing Zenith Angle (VZA). The VZA (represented with  $\alpha$ ) for each pixel is computed according to the satellite VZA algorithms (Gieske et al., 2005) by using general parameters (such as longitude, latitude of each pixel). With the cosine of this angle and the retrieved ash mass loadings ( $M$ ), the mass loadings in the vertical direction ( $M_v$ ) can be calculated by Eq. (1),

$$M_v = M \times \cos(\alpha). \quad (1)$$

To extract ash concentrations from SEVIRI retrievals,  $M_v$  only is not sufficient and knowledge about the vertical distribution of ash cloud must be included. The cloud vertical profile can be described with the height of the top and the thickness of the cloud. As introduced in Section 2, the cloud top height ( $H_{top}$ ) is available from satellite remote sensing and the appropriate thickness range (from  $T_{low}$  to  $T_{high}$ , i.e., 0.2 to 3 km) of the plume has been chosen for this case based on a literature review. Fig. 2 illustrates how the 3D ash concentrations are extracted from the obtained mass loadings in the vertical direction ( $M_v$ ). The blue layer in Fig. 2 is determined by the lowest considered thickness ( $T_{low}$ ) and the target layers used in this study refer to both blue and yellow layers. When the top height and the thickness range of ash cloud are known, the ash concentration in the target layers can be calculated by using the ash mass loadings ( $M_v$ ) at the corresponding

horizontal location. The details are formulated as follows. First we define

$$N_s = \left\lceil \frac{T_{\text{high}} - T_{\text{low}}}{\Delta T} \right\rceil + 1 \quad , \quad (2)$$

$$T_i = T_{\text{low}} + (i - 1) \times \Delta T, \quad C_i = \frac{M_v}{T_i}, \quad i = 1, 2, \dots, N_s \quad , \quad (3)$$

where  $\Delta T$  is a step length and  $N_s$  is the number of the possible thickness.  $T_{\text{low}}$  represents the blue layer (see Fig. 2) with the fixed thickness of 0.2 km and  $T_{\text{high}} - T_{\text{low}}$  (i.e., the subtraction between  $T_{\text{high}}$  and  $T_{\text{low}}$ ) represents the yellow layer with the fixed thickness of 2.8 km.  $\Delta T$  is chosen at a small value compared to  $T_{\text{low}}$ , which guarantees  $N_s$  is not too small (e.g., less than 2) to sample sufficient number of thickness  $T_1, T_2, \dots, T_{N_s}$ . (e.g.,  $\Delta T$  is chosen as 0.05 km in this case study, thus  $N_s$  is calculated as 57.)

Corresponding to the sampled thickness (i.e.,  $T_1, T_2, \dots$ ), the ash concentration can be calculated also as a sample from  $C_1$  to  $C_{N_s}$  through Eq. (3). According to Eq. (2) and Eq. (3),  $T_i$  ( $i = 1, 2, \dots, N_s$ ) is unchanged during the dispersion of the ash cloud, while  $C_i$  is temporally changed but it does not depend on  $H_{\text{top}}$ . Therefore, at one measurement time, the mean ( $C$ ) of the sampled ash concentrations can be calculated by Eq. (4),

$$C = \frac{1}{N_s}(C_1 + C_2 + \dots + C_{N_s}) \quad . \quad (4)$$

$C$  is therefore used in this study as the extracted concentration between the heights [ $H_{\text{top}} - T_{\text{high}}$ ] and  $H_{\text{top}}$  (i.e., both the blue and yellow layers in Fig. 2). ” and we believe this part now has been well improved.

#### Minor/technical comments:

1. *page 2, line 8: “over a long distance”: be more precise and give typical ranges (hundreds of kilometers).*

Response:

Revised as suggested.

2. *page 2, line 27: “there are 3712 ...”: This information is not relevant, more interesting is the spatial resolution (as given later in the paper).*

Response:

Agree. It is removed now.

3. *page 2, line 28: “Nowadays ... as well as the ash cloud top height”: An indication of the accuracy is welcome.*

Response:

As suggested, we have added a note related to this issue in [line\(s\) 5.1–5.3](#):

“ Although there is indeed an error in the ash cloud top height, the product of the errors in the SEVIRI-KNMI ash height has not been available as the product of mass loading errors. Thus, for the current study, we use the data of ash cloud top height as deterministic. ”

4. *page 3, line 10: “mostly from hundreds...”: please rephrase; the thickness is certainly not hundreds of kilometers.*

Response:

Thanks. It is corrected in **line(s) 2.12**:

“ **hundreds of meters** ”

5. *page 3, line 20: “From a modeling perspective...”: The model used in this study should be introduced here (at least earlier than in the current version of the manuscript) and the resolution (and other key parameters) should be mentioned here.*

Response:

I agree with you. Also combined with another reviewer’s comment, the transformation from 2D satellite data to 3D fields is done prior any contact with the model. Thus, this sentence is not suitable here and is removed in the new version. We have re-written this part in **line(s) 3.29–4.5**:

“ For the vertical thickness information of volcanic ash clouds, Schumann et al. (2011) found for the 2010 Eyjafjallajökull eruption using airborne data that the volcanic ash clouds spread over large parts of Central Europe, mostly from hundreds of meters to 3 km depth. This is consistent with the results of (Marenco et al., 2011) who observed layer depths between 0.5 and 3.0 km. Dacre et al. (2015) also examined the ground-based lidar data for the Eyjafjallajökull eruption and found a mean layer depth of  $1.2\pm 0.9$  km and compared this with model based estimates of  $1.1\pm 0.8$  km. Prata and Prata (2012) found variable thicknesses ranging from 0.2 up to 3 km. The vast majority of data suggest thickness in the range 0.2–3 km for the 2010 Eyjafjallajökull eruption. Based on these investigations, it is not realistic to use a deterministic value to represent the overall ash cloud thickness, but we can reasonably assume that the thickness has a range of 0.2–3.0 km at the corresponding horizontal location of the SEVIRI retrieved measurements. Although this thickness information is not deterministic, its uncertainty spread is suitable in an observational operator for satellite data assimilation. Note that the thickness range can be different for other volcanic eruptions. For example, Prata et al. (2015) reported low cloud thickness with 80% of cases for the 2006 Chaiten eruption less than 400 m, thus a thickness range of 0.1–0.4 km is recommended for that eruption. ”

6. *page 3, line 32: “Secondly, using the extracted ...”: What is meant by this statement? What kind of in-situ measurements are used, and where are they from?*

Response:

Here the extracted in situ measurements are meant for the extracted 3D concentrations from 2D mass loadings from SOO. It is re-written in **line(s) 4.16**:

“ Secondly, using the extracted **3D concentrations**, ”

7. *page 4, line 6: "...geographic area affected by the Eyjafjallajökull volcanic ash": The ash affected a larger area than shown, e.g. Spain (Navas-Guzman et al., 2013), Greece (Kokkalis et al., 2013) or Romania (Nemuc et al., 2014). There is also an "European overview" given by Pappalardo et al. (2013). So, the sentence should be more general.*

Response:

Thanks. We have re-written this part in **line(s) 4.23–4.26**:

**" A region covering 30° W to 15° E and 45° N to 70° N is selected here for analysis which includes parts of the geographic areas affected by the Eyjafjallajökull volcanic ash (see Fig. 1). Actually the ash affected a larger area than shown, e.g, Spain (Navas-Guzmán et al., 2013), Greece (Kokkalis et al., 2013), Rominia (Nemuc et al., 2014). There is also an 'European overview' given by Pappalardo et al. (2013). "**

8. *page 4, lines 11 and 14: The statements concerning the error can be combined.*

Response:

Agree. It is revised in **line(s) 4.30–5.1**:

**" Besides ash mass loadings, other products including the ash cloud top height (Fig. 1b), and the error of ash mass loadings (Fig. 1c, which indicates the uncertainty and accuracy of the retrieved mass loadings ) are also available in a near real-time sense (Francis et al., 2012; Prata and Prata, 2012). "**

9. *page 4, line 21: "...resolution to the VATDM resolution": Give numbers for illustration.*

Response:

in **line(s) 5.9–5.11**:

**" Additional processing on the retrieved measurements is needed to translate the data from the original SEVIRI resolution (i.e., 0.1° longitude × 0.1° latitude (Prata and Prata, 2012)) to a VATDM horizontal resolution (i.e., 0.25° longitude × 0.125° latitude, as used in (Fu et al., 2016)). "**

10. *page 4, line 23: "However, the correction cannot...": What is meant with correction; be more precise.*

Response:

It is revised in **line(s) 5.14–5.16**:

**" the correction on the 3D state cannot be directly implemented by DA in the 3D state space due to the insufficient vertical resolution in satellite data (Bocquet et al., 2015). "**

11. *page 4, line 24: "...due to the insufficient vertical resolution in satellite data": This only holds for passive remote sensing. In case of active remote sensing the contrary is true. A comment on this would be welcome.*

Response:

Yes. This is a good point. One comment has been added in **line(s) 5.16–5.21**:

“ Note that this statement only holds for passive remote sensing, e.g., SEVIRI retrievals. In case of active remote sensing the contrary is true. For example, the spaceborne CALIOP lidar certainly has good vertical resolution. In the lower atmosphere it is 30-60 m (below 20 km). The same is true for ground-based lidars but usually these are of limited value. Ceilometers cannot distinguish ash from other scatterers in the lower atmosphere and cloudiness is a big problem – worse than from passive satellite because, at least for the aviation hazard, the ash needs to be elevated (above 10,000 ft or more) and above clouds (a problem then for looking upwards but not for looking downwards). ”

12. *page 6, line 3: It would be appreciated if another name for the “extraction error” is applied. This name does not support the understanding.*

Response:

Yes. We have changed it to “SOO error” which should be to the point.

13. *page 10: In the conclusions two very general comments on future needs/activities are made: “This effective time period probably...” and “How to determine the reasonable ...”. This should be improved by more specific comments. To my knowledge a large number of/most(?) national weather services recently have implemented ceilometer networks, mainly for monitoring the dispersion of volcanic ash clouds (Weigner et al., 2014). These data set will be (and in part are already) available in near real time and will provide excellent information about the (horizontal and) vertical distribution (with some restrictions due to cloud cover; but this is also true for space borne observations). It seems to me that they could be very promising candidates for data assimilation as well, and can complement satellite data.*

Response:

I agree. We have improved the comments more specific to our case study, as in [line\(s\) 12.29–13.2](#):

“ Evaluations using both satellite retrieved data and aircraft in situ measurements showed that the effective forecast time duration after satellite data assimilation with SOO is about 6 hours for the distal part of the Eyjafjallajökull volcanic eruption. The results also showed that the effective forecast duration (after DA with SOO) tends to be longer as the region is farther away from the volcano, which is because inaccurate ESPs require longer time to impact on the regions farther from the volcano. Note that for other cases (e.g., other volcano), this duration should be different and should be re-evaluated due to its dependence on the specific weather condition and on the specific model. ”

In addition, we add comments on the ceilometer networks in the end of the paper in [line\(s\) 13.15–13.20](#):

“ Recently, a large number of national weather services has implemented ceilometer networks, mainly for monitoring the dispersion of volcanic ash clouds (Wiegner et al., 2014). These data set will be (and in part are already) available in near real time and will provide information about the (horizontal and) vertical distribution (with some restrictions due to cloud cover; but this is also true for space borne observations). Thus, they could be promising candidates for data assimilation as well, but there are indeed some caveats. It will be interesting for future research to make use of and demonstrate the case for using ground-based lidars. ”

## Reply to Reviewer #4:

### Major comments:

1. *The authors state that the satellite observations “are often two-dimensional (2D), and cannot easily be combined with a three-dimensional (3D) volcanic ash model”, which motivates their development of a satellite observational operator (SOO). In fact, this issue is common to many DA applications using satellite measurements. Satellite instruments using nadir viewing geometry measure 2D fields. The standard technique in DA is to apply an observational operator (H) to the model output, to be able to compare model and satellite data in measurement space. Satellite observational operators (SOO) are sometimes used to transform observations closer to model space before assimilation. Using an SOO simplifies some aspects of the DA, but does so at the cost of including some set of assumptions in the SOO. In the present case, I find the motivation for the use of a SOO to be lacking (a mismatch between 2D and 3D fields is not sufficient).*

*Furthermore, the assumptions that are included into this SOO appear to be questionable. The authors argue that volcanic ash clouds have thicknesses between 0.5 and 3.0 km, although they quote studies having measured even smaller thicknesses. Given the relative large range, it is not clear why even smaller thicknesses are not included in the range. Then they calculate a range of possible concentrations by dividing the satellite retrieved ash loading (in  $\text{g}/\text{km}^2$ ) by thicknesses between 0.5 and 3.0 km. They take the mean and SD of these concentrations as their best guess (and uncertainty in) ash concentration. This seems like a complicated way of assuming a mean thickness of 1.75 km. Then the authors focus on the ash concentration at cloud top, which appears to be the quantity which is compared to the model output within the DA (although this is not sufficiently explained). There is no real justification for why the focus is restricted to the concentration at cloud top, and this process seems like it discards a significant amount of useful information (e.g., the total mass loading).*

*Most of these assumptions and complications would be avoided if measurements and model results were compared in measurement space rather than model space, as is the standard in DA. This would simply require the observation operator  $H$  to take the vertical integral of the modeled ash profile.*

### Response:

First of all, thank you for pointing out the lack of sufficient motivations. Actually, the motivation to design SOO was not just based on “are often two-dimensional (2D), and cannot easily be combined with a three-dimensional (3D) volcanic ash model”. In the new version, we have carefully and fully introduced the motivations, as in [line\(s\) 3.5–3.23](#):

“ Thus, the 2D measurements are not directly suited in a 3D ensemble-based DA system. One way to ameliorate this difficulty in the analysis step of DA, is to compare the measurements and the model results in the 2D measurement space. This simply requires an observational operator to take the vertical integral of the modeled ash profile. After the analysis in the measurement space, the corrected 2D mass loadings are distributed to each vertical layer based on the prior modeled ash profile. However, this approach adds

artificial vertical correlations to all the vertical ash layers when the prior modeled ash vertical profile is not accurate (Lu et al., 2016b). This is a common problem with respect to passive data assimilation due to the lack of vertical resolution in data (Blayo et al., 2014; Bocquet et al., 2015). For applications where the vertical profile is not an issue (i.e., the prior profile can be modeled well), the added artificial correlations are of minor importance (Blayo et al., 2014). However, this is not the case for volcanic ash application where the ash plume usually has significant vertical variation and is located in a narrow vertical band (e.g., see Fig. 7 in (Prata and Prata, 2012) and Fig. 15(c) in (Lu et al., 2016a)). In general, the used model-based vertical profile is very inaccurate, thus the integral approach cannot accurately reconstruct states for all/most of the vertical ash layers. The influences of the artificial/spurious vertical correlations (introduced by the integral approach with the standard DA) on the assimilation performance has been extensively studied by Lu et al. (2016b) for the volcanic ash application in a concept of variational DA. (In this paper, we also have Section 5 to discuss on this issue with respect to ensemble-based DA).

In this study we look at an approach to avoid the problem of the artificial vertical correlations. Where the satellite provides 2D ash mass loadings, 3D information is available from the model and from additional observations. A 3D Satellite Observational Operator can be derived to make both types of information directly comparable in the 3D model space. This approach does not involve the integral operator, and thus avoids the artificial vertical correlations. ”

In the new version, we have also changed the title to clearly state our approach–

“ Data assimilation for volcanic ash plumes using a Satellite Observational Operator: a case study on the 2010 Eyjafjallajökull volcanic eruption ”

Second, we have considered the smaller thickness in the new version and extended the thickness range to 0.2–3 km. The details about the thickness are in [line\(s\) 3.29–4.5](#):

“ For the vertical thickness information of volcanic ash clouds, Schumann et al. (2011) investigated on the 2010 Eyjafjallajökull eruption using airborne data that the volcanic ash clouds spread over large parts of Central Europe, mostly from hundreds of meters to 3 km depth. This is consistent with the results of (Marenco et al., 2011) who observed layer depths between 0.5 and 3.0 km. Dacre et al. (2015) also examined the ground-based lidar data for the Eyjafjallajökull eruption and found a mean layer depth of  $1.2 \pm 0.9$  km and compared this with model based estimates of  $1.1 \pm 0.8$  km. Prata and Prata (2012) found variable thicknesses ranging from 0.2 up to 3 km. The vast majority of data suggest thickness in the range 0.2–3 km for the 2010 Eyjafjallajökull eruption. Based on these investigations, it is not realistic to use a deterministic value to represent the overall ash cloud thickness, but we can reasonably assume that the thickness has a range of 0.2–3.0 km at the corresponding horizontal location of the SEVIRI retrieved measurements. Although this thickness information is not deterministic, its uncertainty spread is suitable in an observational operator for satellite data assimilation. Note that the thickness range can be different for other volcanic eruptions. For example, Prata et al. (2015) reported low cloud thickness with 80% of cases for the 2006 Chaiten eruption less than 400 m, thus a thickness range of 0.1–0.4 km is recommended for that eruption. ”

Moreover, I agree (and thanks) that the extraction only at the cloud top would discard a significant amount of information. Since we designed SOO based on the thickness range 0.2–3 km, the extraction should not be restricted to the concentration within 0.2 km, but should be for the concentration within 3 km. In the new version, we have re-written this part in [line\(s\) 6.22–6.23](#):

“ C is therefore used in this study as the extracted concentration between the heights [ $H_{\text{top}}$  -  $T_{\text{high}}$ ] and  $H_{\text{top}}$  (i.e., both the blue and yellow layers in Fig. 2). ”  
and in [line\(s\) 7.14–7.15](#):

“ The outcome of SOO can be considered as preprocessing to the satellite data assimilation system. The extracted data represent the data at the target layers, which can be taken as the data within the 3.0 km layer thickness. ”

Third, I agree that the complications would be avoided if measurements and model results were compared in measurement space. However, as answered before, the integral approach would add artificial vertical correlations, which has been investigated and discussed in literature as severe for volcanic ash application. To clearly state assimilation with SOO to be an effective approach for our application, in the new version, we have also added experiments in a new section (Section 5) to compare and discuss the two approaches (EnSR with SOO and without SOO), as in [line\(s\) 10.1–10.30](#):

“ [Section 5 Discussion and comparison between EnSR with SOO and without SOO](#) ”

We have implemented satellite data assimilation combined with SOO. However, this does not mean in terms of methodology, ensemble-based data assimilation without SOO cannot work. Under that circumstance, applying data assimilation on 2D measurements and 3D concentrations, the operator  $H_k$  in Eq. (A5) does not select the grid cell in  $x(k)$ , but integrates all the vertical grid cells to calculate 2D mass loadings. This approach (denoted EnSR without SOO) would simplify the assimilation by only using 2D mass loadings. Although we focused SOO as a new way (as introduced in the introduction) to deal with satellite 3D data assimilation, the assimilation effects between with and without SOO should be better compared/studied in order to determine whether SOO is an effective approach.

Comparing to the EnSR implementations with SOO in Fig. 5c/ Fig. 6c, the cases of EnSR without SOO are shown in Fig. 5d/ Fig. 6d. Taking the SEVIRI retrieved mass loadings (Fig. 5a/ Fig. 6a) as references, it is revealed that EnSR without SOO performs better than the case without assimilation (Fig. 5b/ Fig. 6b), but worse than EnSR with SOO. One may also want to check the assimilation effect without SOO at the initial analysis time (i.e., 01:00 UTC, 16 May 2010), which is illustrated in Fig. 7. It can be seen that the assimilation difference between with and without SOO is small (by comparing Fig. 7c and 7d). While, at the second analysis time (i.e., 02:00 UTC, 16 May 2010) the results show much bigger differences (between Fig. 7g and Fig. 7h). These results verify and examine the influences of the artificial/spurious vertical correlations (caused by the integral-type of  $H_k$ , see introduction). These influences are examined to be accumulated step by step in our volcanic ash application and must be considered/avoided with respect to an acceptable assimilation result.

Now it is explained for our application why we chose SOO to compare measurements and model results in the model space rather than in the measurement space. Although the complications would be avoided if we do the analysis step in measurement space, however, the assimilation accuracy will then be worse than the case in the 3D model space by using SOO. Note that we perform EnSR without SOO in a standard/general way. We expect the problem of artificial vertical correlations (for volcanic ash plumes) may be partially compensated by employing some diagnostic or correction approaches, as discussed in (Blayo et al., 2014; Houtekamer and Zhang, 2016) for other applications. However, this would add many complications/difficulties to standard EnSR assimilation and whether/how it would work remains unknown (at the moment, no literature has reported on this issue for our



application), and that it would be another research.

In this study, we focus on a way not dealing with the artificial vertical correlations, and we propose SOO by incorporating data and information available. The additional data (e.g., cloud top height and thickness information) are important for SOO, which describes the structure of a volcanic ash plume; we also provide an idea in the sense of incorporating many available measurements. In addition, we expect the SOO can be potentially improved by incorporating more data, but at the moment DA with SOO has shown its advantage than the standard way (without SOO) in dealing with passive satellite data assimilation. ”

2. *Fig 1a shows ash mass loadings from SEVERI, with values between 0 and 5 g/m<sup>2</sup> (although values could be higher). Taking 3 g/m<sup>2</sup> as a typical value, and under the assumption that cloud thicknesses are between 0.5 and 3 km thick (and that concentrations are uniform within the cloud), one would expect typical concentrations between 1-6 mg/m<sup>3</sup>. The SOO extracted measurements in Fig 3a are around an order of magnitude less than this, with most values falling between 0.1-0.6 mg/m<sup>3</sup>. The rough concentrations estimated here (1-6 mg/m<sup>3</sup>) are also more in line with the model results shown in Fig 4. Given the apparent simplicity of the SOO, it should be possible for the reader to gain a quantitative feel for the magnitudes of the concentrations involved. At present, this is not possible. If the SOO is more complicated than I have understood it, then the description needs fair amount more detail.*

Response:

I think that the misunderstanding is due to:

(1) the differences between original mass loadings (M) and the vertical mass loadings (M<sub>v</sub>) (i.e., mass loadings in the vertical direction). The former is illustrated in Fig. 1a, while the latter is calculated by  $M_v = M \times \cos(\text{VZA})$  and is the one directly used for the SOO. Thank you for pointing out this question, which reminds us to explicitly plot the vertical mass loadings (i.e., M<sub>v</sub> in Eq. (1) in Fig. 1d.

(2) because there are values in Fig. 1d as high as 5 and as low as 0 g m<sup>-2</sup> does not mean that 3 g m<sup>-2</sup> is typical. We have carefully checked that the typical value in Fig. 1d could be taken as 1 g m<sup>-2</sup>.

Then under the assumption that cloud thicknesses are between 0.2 and 3 km thick, one would expect the typical concentrations between 0.3–5 mg m<sup>-3</sup>. The SOO extracted measurements in Fig. 3 are around this order of magnitude (about 0.5–4 mg m<sup>-3</sup>).

(In this version, we choose the time 01:00 UTC 16 May 2010 to illustrate the development of SOO, which will be further used/refered for the analysis at this time. ) I agree with you that given the apparent simplicity of SOO, it should be possible for the reader to gain a quantitative feel. We believe the current presentation has improved this aspect.

3. *There is only a small amount of evidence shown to support the conclusion that “satellite data assimilation can force the volcanic ash state to match the satellite observations, and that it improves the forecast of the ash state.” Fig 5 shows a snapshot of ash loadings at a single time, comparing the SEVERI measurements with results from the model with and without assimilation. While the assimilation does seem to correct a rather large bias in the pure model output, it’s not clear that the DA result is better in all locations: while the values over the Netherlands may be more realistic, it appears that the DA results over the west coast of Norway may be underestimated by the DA system. Whether the authors have chosen this single comparison randomly, or if this is a best- or worse-case is not stated.*

*One would expect some overall measure of skill with respect to time and space for such a comparison, in order to gauge the impact of DA.*

Response:

Yes, I agree and understand your concerns. In the new version, without loss of generality, we have shown results at both 12:00 UTC 17 May and 00:00 UTC 18 May. (And in Section 5 we also show the results at 01:00 UTC 16 May, 02:00 UTC 16 May.) The related part is re-written in [line\(s\) 9.19–9.27](#):

“ Based on this consideration, SEVIRI ash mass loadings need to be employed for a further validation. Note that the mass loadings used for this comparison are not the original mass loadings, but the mass loadings in the vertical direction, i.e.,  $M_v$  in Eq. (1) as plotted in Fig. 5a.

During two-days continuously assimilating SEVIRI measurements of the extracted  $PM_{10}$  concentrations, without loss of generality, the analyzed volcanic ash state at 12:00 UTC 17 May/ 00:00 UTC 18 May 2010 is shown in Fig. 5c/ Fig. 6c. The conventional simulation without assimilation is also presented (Fig. 5b/ Fig. 6b), which is currently the commonly used strategy for the simulation of volcanic ash transport (Webley et al., 2012; Fu et al., 2015). It is clear that in almost the entire plume, the mass loadings by EnSR with SOO are in a better agreement with the SEVIRI mass loadings. It can be seen that EnSR with SOO effectively decreases the estimation level compared to the conventional simulation. ”

Moreover, I agree that the DA result is not better in all locations. We have added a note to clearly state that in [line\(s\) 9.30–9.33](#):

“ It should also be noted that while the assimilation does correct a rather large bias in the pure model output, it doesn’t mean that the DA result is better in all locations. For example, in locations around Iceland, the DA doesn’t lead the pure model; At a location ( $-1^\circ W$ ,  $58^\circ N$ ) around England (see Fig. 5a), the simulation without assimilation seems to match better. ”

In addition, we think the word “force” is a very strong word, while what we aim to state is “improvement”. Thus to avoid misleading to readers, we have changed “force” to “improve” and re-written the abstract in [line\(s\) 1.10–1.11](#):

“ The results show that satellite data assimilation with SOO can improve the estimate of volcanic ash state, and that it improves the forecast. ”

and the conclusion in [line\(s\) 12.23–12.24](#):

“ The results showed the assimilation with SOO significantly reduces the estimation level of the conventional simulation. The accuracy of the volcanic ash state was shown to be significantly improved by the assimilation of satellite mass loadings. ”

4. *Apparently, DA has already been shown to improve the forecasting of volcanic ash transport (Fu et al., 2015, 2016). The present study claims to quantify the duration of such improvement. Fig 6 shows a comparison of DA forecast results with in situ airplane measurements. Again, the DA initiation helps to correct for a major over estimation by the model without DA. The authors conclude from this comparison that with initial conditions taken from DA, the “effective duration of the improved regional volcanic ash forecasts is about a half day”, although this is a “conservative” estimate, which is based only on this single case, and is in fact limited by the 15 h duration of the airplane measurements. It’s not clear why the continuous satellite measurements were not used to quantify the duration of the improved forecast. The duration of the skill improvement also likely has much to do with the assumptions regarding the noise added to the plume height estimates. A convincing*

*assessment of the skill duration would require a much more thorough and detailed analysis.*

Response:

Thank you for the comments. I agree that satellite data should be the best to evaluate the effective forecast time duration after DA. We have added experiments and more detailed analysis. The major part of Section 6 has been re-written in [line\(s\) 11.1–12.10](#):

“ [Section 6 Evaluation of the effective forecast duration after satellite data assimilation for the distal part of the Eyjafjallajökull volcano](#)

According to Section 4.3, the accuracy of volcanic ash state is significantly improved by ensemble-based data assimilation after a continuous assimilation period (e.g., two days). Apparently, with the improved state as initialization, an improved forecast can be obtained (Fu et al., 2015). However, it remains unknown how long the improvement on forecasts will last.

To investigate the effective duration of the improved ash forecasts after assimilation, a one-day forecast is performed by initializing EnSR analyzed state (Fig. 6c) at 00:00 UTC 18 May 2010. Fig. 8 shows the forecast results after assimilation (first column in Fig. 8), the SEVIRI retrieved measurements (second column in Fig. 8) and the forecast results without assimilation (third column in Fig. 8). Without loss of generality, 06:00, 12:00 and 18:00 UTC are chosen to evaluate the comparisons over three divided distal regions of interest (denoted R1–R3). Note that we do not evaluate the near-volcano region (i.e., the left part of R1 in Fig. 8a), where the improved forecasts can be quickly influenced by the continuously noisy emissions. Thus it is safe to take the effective forecast duration for the near-volcano region as "zero hour".

For the region R1, the improved forecast after assimilation can last for 6 hours. This is viewed by that at 06:00 UTC, the forecast after assimilation (see R1 in Fig. 8a) is closer to the measurements (R1 in Fig. 8b) than the forecast without assimilation (R1 in Fig. 8c). However, the improvement diminishes after 6 hours (see the second and third rows in Fig. 8).

For the region R2, the forecast after DA at 06:00/12:00 UTC ( R2 in Fig. 8a/ 8d) has a good match with the retrieved mass loadings (R2 in Fig. 8b/ 8e). However, we are not sure whether the good match remains at the time 18:00 UTC, because there seems to be lack of data at that time (see R2 in Fig. 8h). Therefore, it is better to evaluate the effective forecast duration after DA with SOO for R2 is 12 hours.

For the region R3, at the three times 06:00/12:00/18:00 UTC, the forecasts after DA are generally better than forecasts without DA by comparing with the measurements. However it should be noted that in Fig. 8e, some higher values (over  $3.5 \text{ g m}^{-2}$ ) are indeed retrieved in R3, but not in the forecasts after DA.

Our initial experimental tests show that, the effective time durations of the forecasts after satellite data assimilation with SOO can be considered as 6 hours for the region R1, 12 hours for the region R2, and 18 hours for the region R3. It also shows to us that the effective forecast duration tends to be longer as the region is farther away from the volcano. This is because longer time is needed for the influences of inaccurate ESPs to reach the areas farther from the volcano.

These results are evaluated using satellite retrieved data. For a further test, we employ another type of independent data. For this purpose, we use aircraft-based measurements (see details in Appendix B). Fig. 9a shows the flight route of the aircraft (in the region R3).

Fig. 9b and 9c are the comparison of aircraft PM<sub>10</sub> measurements against the forecasted concentrations after assimilation and without assimilation. Note that the low magnitude of aircraft measurements may result in little importance to verify high ash concentrations, but comparisons using them can indicate how good the assimilation is at reconstructing the outskirts/boundaries of the ash plume, which is important to describe the plume's structure.

For the period from 09:30 to 11:00 UTC (Fig. 9b), although the forecasting time has been over 9 hours (i.e., the last assimilation is 9 hours ago), the forecasted concentrations still have a good match with the accurate aircraft measurements, while the conventional forecast (i.e., forecast without assimilation) doesn't. This result shows the forecast over 11 hours after assimilation has also kept a high accuracy compared to the measurements. The result can be extended to 15 hours comparing with the other period from 12:30 to 15:00 UTC (Fig. 9c). This test result using independent aircraft data confirms our evaluation result using satellite data that for the region R3, the effective forecast duration after DA is about 18 hours.

Based on all of the above evaluations and in the view of the whole distal regions of interest (R1+R2+R3), 6 hours can be taken as the a reasonable effective time duration (after assimilation with SOO) for the case study. This time duration can be taken as an indication about how long a valid regional aviation advice based on the forecast after assimilation can last. It should be noted that for other cases (e.g., another volcanic eruption), the effective duration is different because it depends on the specific weather condition and the specific model used for forecasting. Thus, the effective duration for other case studies should be re-evaluated, and what we presented in this section can be useful for the readers to test it.

According to the tests, 6 hours can be taken as a reasonable effective time duration for this case. We have re-written this in abstract in [line\(s\) 1.11–1.14](#):

“ Comparison with both satellite retrieved data and aircraft in situ measurements shows that the effective duration of the improved volcanic ash forecasts for the distal part of the Eyjafjallajökull volcano is about 6 hours. ”

and in conclusion in [line\(s\) 12.29–13.2](#):

“ Evaluations using both satellite retrieved data and aircraft in situ measurements showed that the effective forecast time duration after satellite data assimilation with SOO is about 6 hours for the distal part of the Eyjafjallajökull volcanic eruption. The results also showed that the effective forecast duration (after DA with SOO) tends to be longer as the region is farther away from the volcano, which is because inaccurate ESPs require longer time to impact on the regions farther from the volcano. Note that for other cases (e.g., other volcano), this duration should be different and should be re-evaluated due to its dependence on the specific weather condition and on the specific model. ”

We believe this part has been improved compared to the previous presentation.

#### Specific comments:

1. P1, L1: “Data assimilation” is very general, the focus on ash forecasting should be clearer.

Response:

I agree. We have clearly mentioned the focus and re-written the sentence in [line\(s\) 1.1–1.2](#):  
“ Using data assimilation (DA) to improve model forecast accuracy is a powerful approach that requires available observations. ”

2. *P1, L5: It doesn't appear that cloud thickness \*data\* is being included in the DA. Data-based assumptions, maybe.*

Response:

Agree. It is corrected in [line\(s\) 1.6–1.7](#):

“ By integrating available data of ash mass loadings and cloud top heights, and data-based assumptions on thickness, ”

3. *P2, l4: A number of eruption source parameters are mentioned here, but only plume height is included in the DA ensemble generation. Some discussion would be nice at the end of the paper on the potential impact of uncertainties in the other ESPs.*

Response:

This is a good suggestion. The Mass Eruption Rate (MER) is actually uncertain in this study as PH, which is clearly mentioned in [line\(s\) 8.13–8.16](#):

“ Note that in this study the Mass Eruption Rate (MER) is calculated based on each uncertain PH, by using an empirical relationship (Mastin et al., 2009) between PH(km) and MER ( $\text{kg s}^{-1}$ )

$$\text{PH} = 2.00V^{0.241}, \quad \text{and} \quad \frac{V}{\text{MER}} = \frac{1.5e^3}{4.0e^6}. \quad (7)$$

Therefore, although we only add uncertainties in PH, MER is also not deterministic. ”

According to suggestions, we add some discussion on the potential impact of uncertainties in other ESPs, e.g., Vertical Mass Distribution (VMD) and Particle Size Distribution (PSD) in [line\(s\) 13.5–13.11](#):

“ In this study, two of the Eruption Source Parameters (ESPs)–Plume Height (PH) and Mass Eruption Rate (MER) are made uncertain to generate DA ensembles. Actually the uncertainties can also be added in other ESPs, e.g., Vertical Mass Distribution (VMD) and Particle Size Distribution (PSD). However, adding noise in VMD and PSD should be very careful to keep their empirical/realistic distribution, e.g., “umbrella” shaped VMD (Sparks et al., 1997) and PSD for different types of eruption (Durant and Rose, 2009). Otherwise, the noisy VMD or PSD could provide unphysically biased prior ensemble plumes, resulting in DA algorithm impossible to reconstruct physical plume estimates. ”

4. *P2, l10: Actually, you would hope that the VATDM was fairly accurate, and the DA was used because of unknowns in the ESPs.*

Response:

Agree. It is corrected in [line\(s\) 2.13–2.14](#):

“ For the purpose of improving the forecast accuracy of volcanic ash concentrations, efficient solutions must be employed to compensate the ESPs' inaccuracies. ”

5. *P2, l11: DA does more than provide the initial conditions.*

Response:

I agree. It is re-written in [line\(s\) 2.14–2.16](#):

“ Data assimilation (DA) can be used to create accurate initial conditions for model runs by using available measurements, which is one of the most commonly used approaches for real-time forecasting problems (Evensen, 2003; Bocquet et al., 2015; Fu et al., 2015). ”

6. *P2, l17: It’s not clear if these measurements are specific to Eyjafjallajökull, or more general.*

Response:

Here, we mention these measurements specific for the Eyjafjallajökull eruption. It is now clearly mentioned in [line\(s\) 2.20–2.22](#):

“ For the 2010 Eyjafjallajökull volcanic eruption, during volcanic ash transport, different types of scientific measurement campaigns were performed to collect information of the ash plume. ”

7. *P2, l25: should mention that the satellite is geostationary here.*

Response:

Thanks. It is mentioned in [line\(s\) 2.28–2.29](#):

“ Geostationary satellite measurements are of special interest, because the detection domain is large and the output data is at high temporal frequency (typically 15 – 30 minutes). ”

8. *P2, l26: Earth’s*

Response:

Corrected.

9. *P3, l6: Following from general comment, sparseness of data is not a real impediment to its use in DA, in fact, one could argue that sparse data is exactly what DA is useful for!*

Response:

I agree. It is re-written in [line\(s\) 3.26–3.27](#):

“ Cloud-Aerosol Lidar with Orthogonal Polarization (CALIOP) (Winker et al., 2012) lidar measurements can provide detailed vertical information on plumes, but the measurements have low temporal resolution (polar-orbit) and the data processing and delivery are not designed for near real-time applications. ”

10. *P3, l9: This discussion seems to assume that ash clouds have very well defined edges, but could there not be cases where the ash concentration decays smoothly over some vertical range? How is the thickness defined in such cases?*

Response:

Thanks for the question. We have answered it in [line\(s\) 4.7–4.13](#):

“ Layering is a typical property for distal volcanic ash cloud, thus the ash cloud is often called an ash plume. This property results in that usually there are clear edges around the plume, but it could indeed happen that the ash concentration decays smoothly over some vertical range, resulting in unclear ash cloud edges. In these cases, there would be long tails of very low concentrations, but the reported thickness ranges from literature can also fit, because (1) the reported thickness ranges are actually based on the visible/detectable ranges of the ash clouds, which means the observed plume edges do not exactly represent the “zero” concentration edges, but the “detectable” edges; (2) very low concentration is not of interest with respect to air-safety in volcanic ash application. ”

11. *P3,l10: “hundreds of meters”*
12. *P3, l16: “Kasatochi”*
13. *P3, l16: Personal communication should probably list from whom the information is from.*
14. *P3, l21: Whether thin ash clouds are less of a concern to aviation or not does not necessarily make them less of a concern for a data assimilation system.*

Responses to 11, 12, 13, 14:

Thanks for the corrections and comments. We agree. In the new version, we have considered the thin ash clouds by updating the thickness range of 0.5–3.0 to 0.2–3.0 km, based on the literatures for the volcano Eyjafjallajökull. Since we focus on the case study of the volcano Eyjafjallajökull, some irrelevant literature have been removed. We have re-written this part in [line\(s\) 3.29–4.5](#):

“ For the vertical thickness information of volcanic ash clouds, Schumann et al. (2011) investigated on the 2010 Eyjafjallajökull eruption using airborne data that the volcanic ash clouds spread over large parts of Central Europe, mostly from hundreds of meters to 3 km depth. This is consistent with the results of (Marenco et al., 2011) who observed layer depths between 0.5 and 3.0 km. Dacre et al. (2015) also examined the ground-based lidar data for the Eyjafjallajökull eruption and found a mean layer depth of  $1.2\pm 0.9$  km and compared this with model based estimates of  $1.1\pm 0.8$  km. Prata and Prata (2012) found variable thicknesses ranging from 0.2 up to 3 km. The vast majority of data suggest thickness in the range 0.2–3 km for the 2010 Eyjafjallajökull eruption. Based on these investigations, it is not realistic to use a deterministic value to represent the overall ash cloud thickness, but we can reasonably assume that the thickness has a range of 0.2–3.0 km at the corresponding horizontal location of the SEVIRI retrieved measurements. Although this thickness information is not deterministic, its uncertainty spread is suitable in an observational operator for satellite data assimilation. Note that the thickness range can be different for other volcanic eruptions. For example, Prata et al. (2015) reported low cloud thickness with 80% of cases for the 2006 Chaiten eruption less than 400 m, thus a thickness range of 0.1–0.4 km is recommended for that eruption. ”

15. *P4, l12: “As a parameter...” The meaning of this sentence is hard to understand.*

Response:

Yes. It is re-written in [line\(s\) 4.32–5.1](#):

“ The ash cloud top height is adopted with the SEVIRI-KNMI product of ash height, which has been evaluated with a reasonable accuracy, as reported by de Laat and van der A (2012). ”

16. *P4, l15: Also unclear, in the previous paragraph a number of data are described as SEVIRI products.*

Response:

Yes, it is re-written in [line\(s\) 5.4–5.5](#):

“ We acquire the data (described above) from the European Space Agency (ESA) funded project – Volcanic Ash Strategic Initiative Team (VAST). The data are illustrated in Fig. 1. ”

17. *P5, l25: “ML\_blue” is not an intuitive terminology, something physically motivated would be much better.*

Response:

Agree. In the new version, we don’t restrict the extraction at only the blue layer, but extend it to both the blue and yellow layers. Thus, there is no need to specifically represent “ML\_blue”.

18. *P6, Eq. 7: Where does this formula come from? Usually, uncorrelated errors add in quadrature. On line 13, a “conditional probability relation” is mentioned, but this does not make Eq. 7 easier to understand.*

Response:

Based on the comments of another Reviewer, we have re-written this part. The previous formula was developed by us, but not a very convincing formula. We have re-written this formula and this part in [line\(s\) 6.29–7.5](#):

“ Eq. (4) can be written as

$$C = \frac{\cos(\alpha)}{N_s T_1} M + \frac{\cos(\alpha)}{N_s T_2} M + \dots + \frac{\cos(\alpha)}{N_s T_{N_s}} M \quad . \quad (6)$$

Thus, given the standard uncertainty in mass loadings ( $u_M$ , i.e., the data of retrieval error, as shown in Fig. 1c) and according to the theory of combined standard uncertainty (Kirkup and Frenkel, 2006) for uncorrelated errors,  $u_C$  can be calculated by

$$u_C = \sqrt{\left(\frac{\cos(\alpha)}{N_s T_1}\right)^2 + \left(\frac{\cos(\alpha)}{N_s T_2}\right)^2 + \dots + \left(\frac{\cos(\alpha)}{N_s T_{N_s}}\right)^2} \times u_M \quad . \quad (7)$$

Now  $u_C$  is quantified, which together with  $C$  describes the 3D measurements (mean, uncertainties) for ensemble-based data assimilation. ”

19. *P7, l12: This description of the plume height needs much more detail to be understandable.*



Response:

Yes. We have added more details and re-written this part in [line\(s\) 8.6–8.10](#):

“ The PH here represents the eruption height above the vent of the volcano, which was monitored with the weather radar at Keflavik (155 km west of the volcano) by Icelandic Meteorological Office (IMO), sampling every 5 minutes (Gudmundsson et al., 2010). In this study PH is taken based on the maximum detection data of this weather radar (see the Fig. 2a in (Gudmundsson et al., 2010)), and usually the uncertainty of PH is taken as 20 % (Bonadonna and Costa, 2013). ”

20. *P8, l6: “... which is mainly due to lack of sedimentation processes” scared me quite a bit, but Fu et al. (2016) only state that the model contains sedimentation processes, but not coagulation, evaporation and resuspension. I guess assumptions about the size distribution are also important here.*

Response:

Yes, it was not an accurate statement. We have revised it in [line\(s\) 9.8–9.9](#):

“ In reality, a potential overestimation is usually elusive and hard to avoid, which is mainly due to the difficulty in getting an accurate estimation of the particle size distribution and modeling the physical processes (Fu et al., 2016). ”

21. *P8, l7: Using DA to correct for model overestimation is a rather unphysical “solution”. It would be more satisfying to improve the physics of the model if in fact this is the source of the over-estimation.*

Response:

Agree. But for our case we actually don’t know what is the exact source for over-estimation. We have added this statement in the new version in [line\(s\) 9.27–9.30](#):

“ Note that using DA to correct for model over-estimation is an unphysical “solution”. It would be more satisfying to improve the physics of the model if in fact this is the source of the over-estimation, but for this case we don’t know what is the exact source (which could be e.g., meteorology, ESPs, model processes). ”

22. *P8, l26: This is not a very convincing validation of the SOO.*

Response:

I agree. It is not a suitable statement and has been removed.

23. *P8, l27: Is there a reason why SEVIRI mass loading retrieval error and the standard deviation of the mass loadings should be similar? The reason is not apparent.*

Response:

I agree with you that the reason is not apparent, and actually there is no specific reason for it. This is also why we checked both to see the differences. Since only the retrieval error is (while the standard deviation of the mass loadings is not) relevant to the study, thus the statement on this check is not very relevant to the study. To avoid unclear information, in

the new version, we have removed this sentence.

24. *P9, l3: I don't see why satellite measurements wouldn't be better to test the duration of improvements to forecasts from DA. That satellite measurements have "big uncertainties" seems a strange argument, given that the preceding portions of the paper have used satellite measurements for the DA. While I don't mean to play down the importance of in situ measurements, in this case, the airplane flight track sampled only the very edges of the old ash plume, with concentrations orders of magnitude less than the peak values and much lower than the threshold for airplane safety. Therefore, the accuracy of the forecasts at the times and places of the in situ data used here seem to be of little importance to the question of how good the model is at predicting ash concentrations dangerous to airplanes.*

Response:

Thank you for the comments and explanations, which helps improve the presentation of this part. We have answered this question in the Major concern 4. We agree that satellite measurements should be better to test the duration than the aircraft measurements. In the new version, we use both for the test. Although the low magnitude of aircraft measurements may result in little importance to verify high ash concentrations, but comparisons using them can indicate how good the assimilation is at reconstructing the outskirts/boundaries of the ash plume, which is important to describe the plume's structure. Thus, we kept the usage of them as a second test after the main test with satellite data, and also mentioned this in [line\(s\) 11.30–11.32](#):

“ Note that the low magnitude of aircraft measurements may result in little importance to verify high ash concentrations, but comparisons using them can indicate how good the assimilation is at reconstructing the outskirts/boundaries of the ash plume, which is important to describe the plume's structure. ”

The revised manuscript starts from next page.

# Data assimilation for volcanic ash plumes using a Satellite Observational Operator: a case study on the 2010 Eyjafjallajökull volcanic eruption

Guangliang Fu<sup>1</sup>, Fred Prata<sup>2</sup>, Hai Xiang Lin<sup>1</sup>, Arnold Heemink<sup>1</sup>, Arjo Segers<sup>3</sup>, and Sha Lu<sup>1</sup>

<sup>1</sup>Delft University of Technology, Delft Institute of Applied Mathematics, Mekelweg 4, 2628 CD Delft, The Netherlands.

<sup>2</sup>Nicarnica Aviation AS, Gunnar Randers vei 24, NO-2007 Kjeller, Norway.

<sup>3</sup>TNO, Department of Climate, Air and Sustainability, P.O. Box 80015, 3508 TA Utrecht, The Netherlands.

*Correspondence to:* Guangliang Fu (G.Fu@tudelft.nl)

**Abstract.** Using data assimilation (DA) to improve model forecast accuracy is a powerful approach that requires available observations. Infrared satellite measurements of volcanic ash mass loadings are often used as input observations for the assimilation scheme. However, because these primary satellite-retrieved data are often two-dimensional (2D) and the ash plume is usually vertically located in a narrow band, thus directly assimilating the 2D ash mass loadings in a three-dimensional (3D) volcanic ash model (with an integral observational operator) can usually introduce large artificial/spurious vertical correlations.

In this study, we look at an approach to avoid the artificial vertical correlations by not involving the integral operator. By integrating available data of ash mass loadings and cloud top heights, and data-based assumptions on thickness, we propose a Satellite Observational Operator (SOO) that translates satellite-retrieved 2D volcanic ash mass loadings to 3D concentrations. The 3D SOO makes the analysis step of assimilation comparable in the 3D model space.

Ensemble-based data assimilation is used to assimilate the extracted measurements of ash concentrations. The results show that satellite data assimilation with SOO can improve the estimate of volcanic ash state and the forecast. Comparison with both satellite retrieved data and aircraft in situ measurements shows that the effective duration of the improved volcanic ash forecasts for the distal part of the Eyjafjallajökull volcano is about 6 hours.

## 1 Introduction

It has been known for many years that volcanic ash is dangerous to commercial jet aircraft (Casadevall, 1994). Little is known about the exact level of ash concentrations that becomes dangerous to the jet turbine, and the current recommendation states that the highest concentration an aircraft can endure is  $4.0 \text{ mg m}^{-3}$  (EASA, 2015). Until carefully designed engine performance tests are conducted in realistic volcanic ash cloud conditions, a cautious approach to advising commercial jet operations in airspace is recommended. As a consequence, the eruption of the Eyjafjallajökull volcano in Iceland from 14 April to 25 May 2010, caused an unprecedented closure of the European and North Atlantic airspace resulting in a huge global economic loss of up to 5 billion US dollars (Oxford-Economics, 2010). Due to the major impacts on the aviation community, a lot of research

has been initiated on how to efficiently reduce these aviation impacts, starting with improving the accuracy of volcanic ash forecasts after eruption onset (Eliasson et al., 2011; Schumann et al., 2011).

For forecasting volcanic ash plumes, many Volcanic Ash Transport and Dispersion Models (VATDM) are worldwide available, e.g., PUFF (Searcy et al., 1998), HYSPLIT (Draxler and Hess, 1998), ATHAM (Oberhuber et al., 1998), NAME (Jones et al., 2007) and LOTOS-EUROS (Fu et al., 2015). Literatures have reported in-depth comparisons between volcanic ash real-time advisories and volcanic ash transport models (Witham et al., 2007; Webley et al., 2012). The meteorological wind fields and estimates of Eruption Source Parameters (ESPs) such as Plume Height (PH), Mass Eruption Rate (MER), Particle Size Distribution (PSD) and Vertical Mass Distribution (VMD) are necessary as inputs to the VATDM (Mastin et al., 2009). A VATDM uses physical parameterizations of particle sources and removal processes (including sedimentation and deposition) that affect the concentrations in a dispersing volcanic plume. Without accurate knowledge of the ash removal rate in atmospheres and the temporal variation of MER at the volcano, it is impossible to provide quantitatively accurate concentration forecasts for the ash plume arriving in an airspace over **hundreds of kilometers** (Prata and Prata, 2012; Fu et al., 2016).

For the purpose of improving the forecast accuracy of volcanic ash concentrations, efficient solutions must be employed to compensate the **ESPs' inaccuracies**. **Data assimilation (DA) can be used to create accurate initial conditions for model runs by using available measurements, which is one of the most commonly used approaches for real-time forecasting problems (Evensen, 2003; Bocquet et al., 2015; Fu et al., 2015)**. In each assimilation step, a forecast from the previous model simulation is used as a first guess, then available observations are used to modify this forecast in better agreement with these observations. An important aspect of the assimilation approach is that it reduces the dependency on accurate knowledge of the ESPs – which are generally unknown at the time of an eruption. This is an effective approach where valid real-time volcanic ash measurements are required to guarantee the forecast accuracy (Fu et al., 2015). **For the 2010 Eyjafjallajökull volcanic eruption, during volcanic ash transport, different types of scientific measurement campaigns were performed to collect information of the ash plume**. The measurements contained e.g., ground-based lidar and ceilometer measurements (Pappalardo et al., 2010; Wiegner et al., 2012), **satellite observations (Stohl et al., 2011; Prata and Prata, 2012)**, aircraft-based measurements (Schumann et al., 2011; Weber et al., 2012; Schäfer et al., 2011), ground-based in situ measurements (Emeis et al., 2011), balloon measurements (Flentje et al., 2010) and ground-based remote sensing Sun photometer observations (Ansmann et al., 2010). However, it should be noted that such measurements usually are not available globally and for remote volcanoes it is usually hard to perform measurement campaigns, especially as consequence of sudden eruptions.

**Geostationary satellite measurements are of special interest, because the detection domain is large and the output data is at high temporal frequency (typically 15 - 30 minutes)**. For example, the Spin Enhanced Visible and Infrared Imager (SEVIRI), on board the Meteosat Second Generation (MSG) platform provides a large view coverage of the atmosphere and **Earth's surface (Schmetz et al., 2002)**. **Images can be acquired every 15 minutes**. These satellite data have been used for many years to retrieve ash mass loadings in a dispersing volcanic plume (Prata and Prata, 2012). Nowadays, ash mass loadings (Prata and Prata, 2012), the effective particle size (Kylling et al., 2015) as well as the ash cloud top height (Francis et al., 2012), are available in near real-time as satellite products during volcanic plume transport. The availability of satellite-based data provides

us with an opportunity to employ ensemble-based data assimilation with a VATDM to continuously correct the volcanic ash state, and then improve the forecast accuracy of volcanic ash concentrations.

There still exist difficulties on how to efficiently use volcanic ash mass loadings, because a VATDM is in most cases a 3D model, while the satellite-retrieved ash mass loadings are 2D data. One 2D mass loading can be considered as an integral of ash concentrations along a retrieval path (Prata and Prata, 2012). Thus, the 2D measurements are not directly suited in a 3D ensemble-based DA system. One way to ameliorate this difficulty in the analysis step of DA, is to compare the measurements and the model results in the 2D measurement space. This simply requires an observational operator to take the vertical integral of the modeled ash profile. After the analysis in the measurement space, the corrected 2D mass loadings are distributed to each vertical layer based on the prior modeled ash profile. However, this approach adds artificial vertical correlations to all the vertical ash layers when the prior modeled ash vertical profile is not accurate (Lu et al., 2016b). This is a common problem with respect to passive data assimilation due to the lack of vertical resolution in data (Blayo et al., 2014; Bocquet et al., 2015). For applications where the vertical profile is not an issue (i.e., the prior profile can be modeled well), the added artificial correlations are of minor importance (Blayo et al., 2014). However, this is not the case for volcanic ash application where the ash plume usually has significant vertical variation and is located in a narrow vertical band (e.g., see Fig. 7 in (Prata and Prata, 2012) and Fig. 15(c) in (Lu et al., 2016a)). In general, the used model-based vertical profile is very inaccurate, thus the integral approach cannot accurately reconstruct states for all/most of the vertical ash layers. The influences of the artificial/spurious vertical correlations (introduced by the integral approach with the standard DA) on the assimilation performance has been extensively studied by Lu et al. (2016b) for the volcanic ash application in a concept of variational DA. (In this paper, we also have Section 5 to discuss on this issue with respect to ensemble-based DA).

In this study we look at an approach to avoid the problem of the artificial vertical correlations. Where the satellite provides 2D ash mass loadings, 3D information is available from the model and from additional observations. A 3D Satellite Observational Operator can be derived to make both types of information directly comparable in the 3D model space. This approach does not involve the integral operator, and thus avoids the artificial vertical correlations. For this purpose, vertical information of the ash cloud, such as the ash cloud top height (de Laat and van der A, 2012), the cloud thickness and the corresponding uncertainties, should be included. Cloud-Aerosol Lidar with Orthogonal Polarization (CALIOP) (Winker et al., 2012) lidar measurements can provide detailed vertical information on plumes, but the measurements have low temporal resolution (polar-orbit) and the data processing and delivery are not designed for near real-time applications. Thus CALIOP data is not suitable to provide the near real-time thickness information for the overall volcanic ash plume.

For the vertical thickness information of volcanic ash clouds, Schumann et al. (2011) found for the 2010 Eyjafjallajökull eruption using airborne data that the volcanic ash clouds spread over large parts of Central Europe, mostly from hundreds of meters to 3 km depth. This is consistent with the results of (Marenco et al., 2011) who observed layer depths between 0.5 and 3.0 km. Dacre et al. (2015) also examined the ground-based lidar data for the Eyjafjallajökull eruption and found a mean layer depth of  $1.2 \pm 0.9$  km and compared this with model based estimates of  $1.1 \pm 0.8$  km. Prata and Prata (2012) found variable thicknesses ranging from 0.2 up to 3 km. The vast majority of data suggest thickness in the range 0.2–3 km for the 2010 Eyjafjallajökull eruption. Based on these investigations, it is not realistic to use a deterministic value to represent the overall

ash cloud thickness, but we can reasonably assume that the thickness has a range of 0.2–3.0 km at the corresponding horizontal location of the SEVIRI retrieved measurements. Although this thickness information is not deterministic, its uncertainty spread is suitable in an observational operator for satellite data assimilation. Note that the thickness range can be different for other volcanic eruptions. For example, Prata et al. (2015) reported low cloud thickness with 80% of cases for the 2006 Chaiten eruption less than 400 m, thus a thickness range of 0.1–0.4 km is recommended for that eruption. Another note is that we are only considering the distal plume, at least the part >100 km's from source, which is because close to the emission source the layering of volcanic ash did not necessarily take place. Layering is a typical property for distal volcanic ash cloud, thus the ash cloud is often called an ash plume. This property results in that usually there are clear edges around the plume, but it could indeed happen that the ash concentration decays smoothly over some vertical range, resulting in unclear ash cloud edges. In these cases, there would be long tails of very low concentrations, but the reported thickness ranges from literature can also fit, because (1) the reported thickness ranges are actually based on the visible/detectable ranges of the ash clouds, which means the observed plume edges do not exactly represent the “zero” concentration edges, but the “detectable” edges; (2) very low concentration is not of interest with respect to air-safety in volcanic ash application.

In this paper we focus on the case study of the Eyjafjallajökull volcanic ash plume in May 2010. In order to integrate data and information about volcanic ash clouds, the first goal in this study is to develop a Satellite Observational Operator to translate satellite-retrieved 2D ash mass loadings to 3D concentrations. Secondly, using the extracted 3D concentrations, we investigate whether ensemble-based data assimilation can significantly improve the volcanic ash state. Finally, the effective duration of the improved volcanic ash forecasts after satellite data assimilation is quantified.

## 2 Available data for data assimilation

In this study, geostationary SEVIRI observations for the 2010 Eyjafjallajökull volcanic eruption plume (Prata and Prata, 2012) are used as the study case to design a suitable Satellite Observational Operator (SOO) for DA. SEVIRI is a 12-channel spin-stabilized imaging radiometer. Measurements are made with a spatial resolution from 3 km × 3 km at the sub-satellite point to 10 km × 10 km at the edges of the scan. A region covering 30° W to 15° E and 45° N to 70° N is selected here for analysis which includes parts of the geographic areas affected by the Eyjafjallajökull volcanic ash (see Fig. 1). Actually the ash affected a larger area than shown, e.g, Spain (Navas-Guzmán et al., 2013), Greece (Kokkalis et al., 2013), Rominia (Nemuc et al., 2014). There is also an ‘European overview’ given by Pappalardo et al. (2013).

The main retrieval products from SEVIRI are ash mass loadings (Prata and Prata, 2012; Kylling et al., 2015) (see Fig. 1a, value at 0 means no data) where 01:00 UTC 16 May 2010 is chosen for the illustration, without loss of generality. The mass loading at each 2D pixel gives information on the ash cloud from the top view (Prata and Prata, 2012), which can be taken as an integration of ash concentrations along the retrieval path. Besides ash mass loadings, other products including the ash cloud top height (Fig. 1b), and the error of ash mass loadings (Fig. 1c, which indicates the uncertainty and accuracy of the retrieved mass loadings ) are also available in a near real-time sense (Francis et al., 2012; Prata and Prata, 2012). The ash cloud top height is adopted with the SEVIRI-KNMI product of ash height, which has been evaluated with a reasonable accuracy, as reported by

de Laat and van der A (2012). Although there is indeed an error in the ash cloud top height, the product of the errors in the SEVIRI-KNMI ash height has not been available as the product of mass loading errors. Thus, for the current study, we use the data of ash cloud top height as deterministic.

We acquire the data (described above) from the European Space Agency (ESA) funded project – Volcanic Ash Strategic Initiative Team (VAST). The data are illustrated in Fig. 1. The VAST retrieval utilizes two techniques: 1) A rudimentary cloud detection scheme implemented in the Eumetsat operational scheme called “VOLE” (<http://navigator.eumetsat.int/discovery/Start/DirectSearch/DetailResult.do?f%28r0%29=EO:EUM:DAT:MSG:VOLE>), and 2) A more complex scheme called CID (Cloud Identification). This scheme is described in an Algorithm Theoretical Basis Document (ATBD) (unpublished but available here: (<http://vast.nilu.no/satellite-observations/>)). We have used retrievals from the CID scheme. Additional processing on the retrieved measurements is needed to translate the data from the original SEVIRI resolution (i.e.,  $0.1^\circ$  longitude  $\times$   $0.1^\circ$  latitude (Prata and Prata, 2012)) to a VATDM horizontal resolution (i.e.,  $0.25^\circ$  longitude  $\times$   $0.125^\circ$  latitude, as used in (Fu et al., 2016)).

Limited validation has shown that the satellite ash retrievals are sufficiently accurate for use with dispersion models to correct ash concentration forecasts (Prata and Prata, 2012; Kylling et al., 2015). However, the correction on the 3D state cannot be directly implemented by DA in the 3D state space due to the insufficient vertical resolution in satellite data (Bocquet et al., 2015). Note that this statement only holds for passive remote sensing, e.g., SEVIRI retrievals. In case of active remote sensing the contrary is true. For example, the spaceborne CALIOP lidar certainly has good vertical resolution. In the lower atmosphere it is 30-60 m (below 20 km). The same is true for ground-based lidars but usually these are of limited value. Ceilometers cannot distinguish ash from other scatterers in the lower atmosphere and cloudiness is a big problem – worse than from passive satellite because, at least for the aviation hazard, the ash needs to be elevated (above 10,000 ft or more) and above clouds (a problem then for looking upwards but not for looking downwards).

### 3 Satellite Observational Operator (SOO)

#### 3.1 Derivation

The derivation of the Satellite Observational Operator (SOO) is shown in Fig. 2. The retrieved values by SEVIRI for the ash mass loadings ( $M$ ) can be taken as an integration of ash concentrations along the retrieval path. In principle, the satellite retrieval path could be complicated but generally it is assumed to be a straight line (along the line-of-sight, ignoring refraction) from the measuring apparatus. The angle between the local zenith and the line of sight to the satellite is called Viewing Zenith Angle (VZA). The VZA (represented with  $\alpha$ ) for each pixel is computed according to the satellite VZA algorithms (Gieske et al., 2005) by using general parameters (such as longitude, latitude of each pixel). With the cosine of this angle and the retrieved ash mass loadings ( $M$ ), the mass loadings in the vertical direction ( $M_v$ ) can be calculated by Eq. (1),

$$M_v = M \times \cos(\alpha). \quad (1)$$

To extract ash concentrations from SEVIRI retrievals,  $M_v$  only is not sufficient and knowledge about the vertical distribution of ash cloud must be included. The cloud vertical profile can be described with the height of the top and the thickness of the cloud. As introduced in Section 2, the cloud top height ( $H_{\text{top}}$ ) is available from satellite remote sensing and the appropriate thickness range (from  $T_{\text{low}}$  to  $T_{\text{high}}$ , i.e., 0.2 to 3 km) of the plume has been chosen for this case based on a literature review.

Fig. 2 illustrates how the 3D ash concentrations are extracted from the obtained mass loadings in the vertical direction ( $M_v$ ). The blue layer in Fig. 2 is determined by the lowest considered thickness ( $T_{\text{low}}$ ) and the target layers used in this study refer to both blue and yellow layers. When the top height and the thickness range of ash cloud are known, the ash concentration in the target layers can be calculated by using the ash mass loadings ( $M_v$ ) at the corresponding horizontal location. The details are formulated as follows. First we define

$$N_s = \left\lceil \frac{T_{\text{high}} - T_{\text{low}}}{\Delta T} \right\rceil + 1, \quad (2)$$

$$T_i = T_{\text{low}} + (i - 1) \times \Delta T, \quad C_i = \frac{M_v}{T_i}, \quad i = 1, 2, \dots, N_s, \quad (3)$$

where  $\Delta T$  is a step length and  $N_s$  is the number of the possible thickness.  $T_{\text{low}}$  represents the blue layer (see Fig. 2) with the fixed thickness of 0.2 km and  $T_{\text{high}} - T_{\text{low}}$  (i.e., the subtraction between  $T_{\text{high}}$  and  $T_{\text{low}}$ ) represents the yellow layer with the fixed thickness of 2.8 km.  $\Delta T$  is chosen at a small value compared to  $T_{\text{low}}$ , which guarantees  $N_s$  is not too small (e.g., less than 2) to have a sufficient number of sample thickness  $T_1, T_2, \dots, T_{N_s}$ . (e.g.,  $\Delta T$  is chosen as 0.05 km in this case study, thus  $N_s$  is calculated as 57.)

Corresponding to the sampled thickness (i.e.,  $T_1, T_2, \dots$ ), the ash concentration can be calculated also as a sample from  $C_1$  to  $C_{N_s}$  through Eq. (3). According to Eq. (2) and Eq. (3),  $T_i$  ( $i = 1, 2, \dots, N_s$ ) is unchanged during the dispersion of the ash cloud, while  $C_i$  is temporally changed but it does not depend on  $H_{\text{top}}$ . Therefore, at one measurement time, the mean ( $C$ ) of the sampled ash concentrations can be calculated by Eq. (4),

$$C = \frac{1}{N_s} (C_1 + C_2 + \dots + C_{N_s}) \quad (4)$$

$C$  is therefore used in this study as the extracted concentration between the heights [ $H_{\text{top}} - T_{\text{high}}$ ] and  $H_{\text{top}}$  (i.e., both the blue and yellow layers in Fig. 2).

### 3.2 SOO error

Fig. 2 and Eq. (2) to (4) describe the details of the SOO. The operator transforms the 2D ash mass loadings ( $M$ ) to 3D ash concentrations ( $C$ ). Fig. 3a shows the extracted ash concentrations ( $C$ ) at the target layers. It can be seen that the extracted ash concentrations in the ash plume are mostly between 0.5 and 3.0  $\text{mg m}^{-3}$ .

Now we quantify the standard uncertainty of  $C$  ( $u_C$ , i.e., the SOO error), which is important for a data assimilation system. Eq. (4) can be written as

$$C = \frac{\cos(\alpha)}{N_s T_1} M + \frac{\cos(\alpha)}{N_s T_2} M + \dots + \frac{\cos(\alpha)}{N_s T_{N_s}} M \quad (5)$$



Thus, given the standard uncertainty in mass loadings ( $u_M$ , i.e., the data of retrieval error, as shown in Fig. 1c) and according to the theory of combined standard uncertainty (Kirkup and Frenkel, 2006) for uncorrelated errors,  $u_C$  can be calculated by

$$u_C = \sqrt{\left(\frac{\cos(\alpha)}{N_s T_1}\right)^2 + \left(\frac{\cos(\alpha)}{N_s T_2}\right)^2 + \dots + \left(\frac{\cos(\alpha)}{N_s T_{N_s}}\right)^2} \times u_M \quad . \quad (6)$$

Now  $u_C$  is quantified, which together with  $C$  describes the 3D measurements (mean, uncertainties) for ensemble-based data assimilation.

Note that in this study we discuss the situation that there is an ash plume in clear-sky atmosphere. However, in general there are water and ice clouds above/below/within the ash plume, and situations where clouds move above the ash layer. In such situations the ash plume cannot be detected by the satellite algorithms (Prata and Prata, 2012), leading to wrong assimilation input. For these reasons the SEVIRI retrieval takes a very conservative approach with lots of different thresholds and conditions to be met before a pixel is deemed to be ash-affected. Thus the error is more likely to be towards under-estimating the amount of ash. There is an error associated with the ash retrieval that reflects the confidence of the detection algorithm, as well as the error estimates on the derived quantities. Therefore under these situations, the SOO errors are also more likely to be an under-estimation.

The outcome of SOO can be considered as preprocessing to the satellite data assimilation system. The extracted data represent the data at the target layers, which can be taken as the data within the 3.0 km layer thickness. The other layer thickness is also of high importance, which is used for the derivation of uncertainties.

## 4 Assimilation of satellite-extracted ash concentrations

### 4.1 Satellite data assimilation system

An ensemble-based data assimilation technique is used in this study to assimilate the SEVIRI-based ash concentrations extracted by SOO. After the ensemble Kalman filter was proposed by Evensen (1994), many other algorithms were developed such as the reduced rank square root filter (Verlaan and Heemink, 1997), the ensemble Kalman smoother (Evensen and van Leeuwen, 2000), ensemble square root filter (Evensen, 2004). Ensemble-based data assimilation allows a very general statistical description of errors and is suitable for estimation of concentrations (Evensen, 2003). Based on the ensemble formulation, the dynamical model is not restricted to linearity and the implementation of the algorithm is very simple (Bocquet et al., 2015). The ensemble square root filter (EnSR, see Appendix A), in most applications a more efficient method (Evensen, 2004) than the ensemble Kalman filter, is employed in this study to perform the ensemble-based data assimilation. Note that the observational operator ( $\mathbf{H}$ , see Appendix A) used in EnSR is different from SOO. SOO is an operator designed as a preprocessing procedure before data assimilation, which doesn't depend on the model space and aims to transfer 2D satellite data into 3D measurements for later usage in EnSR. While,  $\mathbf{H}$  is an intrinsic operator in the EnSR algorithm, as specified in Appendix A.

To simulate volcanic ash transport, the LOTOS-EUROS model (Schaap et al., 2008) is used in this study. The configurations and evaluations of the LOTOS-EUROS as a proper volcanic ash transport model was reported by Fu et al. (2015). The model

run starts at 00:00 UTC 15 May 2010 with an initial ash load obtained from previous LOTOS-EUROS model run. As the model state changes with time in the numerical simulation (the time step of the model run is 15 minutes used by Fu et al. (2015)), the model result from the previous time step is taken as the initial state for the next time step. When the model run arrives at 01:00 UTC 16 May, the volcanic ash state gets continuously modified by the data assimilation process until 00:00 UTC 18 May, by combining the extracted measurements of ash concentrations. The specification of uncertainties is essential for a successful data assimilation. Here we use uncertainties in the Plume Height (PH). The PH here represents the eruption height above the vent of the volcano, which was monitored with the weather radar at Keflavík (155 km west of the volcano) by Icelandic Meteorological Office (IMO), sampling every 5 minutes (Gudmundsson et al., 2010). In this study PH is taken based on the maximum detection data of this weather radar (see the Fig. 2a in (Gudmundsson et al., 2010)), and usually the uncertainty of PH is taken as 20 % (Bonadonna and Costa, 2013). The stochastic Plume Height (PH) is assumed to be temporally correlated with exponential decay. The correlation parameter  $\tau$  is set to be 1 hour (Fu et al., 2015). Thus, the PH noise ( $N_{ph}$ ) at two times ( $t_1$  and  $t_2$ ) has the relation (Evensen, 2004) of  $\mathbb{E}[N_{ph}(t_1) \cdot N_{ph}(t_2)] = e^{-\frac{|t_1-t_2|}{\tau}}$ , where  $\mathbb{E}$  represents the mathematical expectation. Note that in this study the Mass Eruption Rate (MER) is calculated based on each uncertain PH, by using an empirical relationship (Mastin et al., 2009) between PH(km) and MER ( $\text{kg s}^{-1}$ )

$$PH = 2.00V^{0.241}, \quad \text{and} \quad \frac{V}{\text{MER}} = \frac{1.5e^3}{4.0e^6}. \quad (7)$$

Therefore, although we only add uncertainties in PH, MER is also not deterministic.

## 4.2 Total measurement error

To assimilate measurements in a simulation model, the total measurement error must be first estimated, which not only contains the SOO error (Section 3.2), but also includes an estimate of the model representation error (Fu et al., 2015). The model representation error is the discrepancy between the measurement location and where the model can represent the measurement. Concentration values are defined on discrete grids with a finite resolution at discrete time steps. The grid resolution of the model used in the study is  $0.25^\circ$  longitude  $\times$   $0.125^\circ$  latitude  $\times$  1 km altitude, while the SEVIRI pixel size here is  $0.1^\circ$  longitude  $\times$   $0.1^\circ$  latitude. After a careful check on the SEVIRI measurements, a measurement location does not coincide with the grid center point where the concentration value is defined. In this study, a preprocessing procedure before data assimilation is employed to average all measurements in a model grid to generate a new measurement value for this model grid. With this approach, one new measurement thus almost corresponds to one model state point, which means the representation error of the model is probably small. For the moment we will therefore not explicitly specify a model representation error, but implicitly assume that it is zero. Therefore, the total measurement error used in data assimilation, is equal to the SOO error in this study.

After the measurements of concentrations are extracted and the total measurement error is quantified, EnSR can be used to combine them with the LOTOS-EUROS model running to reconstruct optimal estimates.

### 4.3 Assimilation performance

In the following, we first examine how data assimilation actually works in the system (see Fig. 4). The first assimilation result with EnSR (Fig. 4a, b), at 01:00 UTC 16 May 2010, is shown against the SEVIRI extracted measurements (Fig. 4c). Ensemble-based data assimilation includes two steps (forecast and analysis, see Appendix A). After one-day of model running started from 00:00 UTC 15 May 2010, the EnSR forecasted state at 01:00 UTC 16 May 2010 is shown in Fig. 4a. Comparing the state to the extracted measurements (Fig. 4c), the former shows a much larger estimation compared to the latter. After the EnSR analysis step (see Fig. 4b), the concentrations in large parts are now closer to the extracted measurements. In reality, a potential overestimation is usually elusive and hard to avoid, which is mainly due to the difficulty in getting an accurate estimation of the particle size distribution and modeling the physical processes (Fu et al., 2016). The comparison between the state of analysis and forecast illustrates that the EnSR assimilation process can potentially solve the problem of overestimation. Note that, in this study only PM<sub>10</sub> ash component is considered in the assimilation system. This is consistent with that (during satellite retrievals) only the fine particles (mostly with sizes <10.0 μm) can be detected in the tropospheric volcanic plume based on the robust and reliable retrieval algorithms (Prata, 1989; Corradini et al., 2008). It is also the main mass fraction that is transported at large distances from the source, since most of the large particles (and therefore mass) is removed quickly from the plume.

The results above were compared in terms of concentrations, not the original mass loadings. To guarantee the assimilation performance, the comparison in concentrations only is not sufficient, because the original data is not concentrations but mass loadings. If SOO is not accurate enough for extracting the concentrations at specified heights, the assimilation results still can approximate well the inaccurate extracted concentrations due to the intrinsic forcing of ensemble-based algorithms. Obviously, the approximation in this case is incorrect. Based on this consideration, SEVIRI ash mass loadings need to be employed for a further validation. Note that the mass loadings used for this comparison are not the original mass loadings, but the mass loadings in the vertical direction, i.e.,  $M_v$  in Eq. (1) as plotted in Fig. 5a.

During two-days continuously assimilating SEVIRI measurements of the extracted PM<sub>10</sub> concentrations, without loss of generality, the analyzed volcanic ash state at 12:00 UTC 17 May/ 00:00 UTC 18 May 2010 is shown in Fig. 5c/ Fig. 6c. The conventional simulation without assimilation is also presented (Fig. 5b/ Fig. 6b), which is currently the commonly used strategy for the simulation of volcanic ash transport (Webley et al., 2012; Fu et al., 2015). It is clear that in almost the entire plume, the mass loadings by EnSR with SOO are in a better agreement with the SEVIRI mass loadings. It can be seen that EnSR with SOO effectively decreases the estimation level compared to the conventional simulation. Note that using DA to correct for model over-estimation is an unphysical “solution”. It would be more satisfying to improve the physics of the model if in fact this is the source of the over-estimation, but for this case we don’t know what is the exact source (which could be e.g., meteorology, ESPs, model processes). It should also be noted that while the assimilation does correct a rather large bias in the pure model output, it doesn’t mean that the DA result is better in all locations. For example, in locations around Iceland, the DA doesn’t lead the pure model; At a location (-1°W, 58°N) around England (see Fig. 5a), the simulation without assimilation seems to match better.

## 5 Discussion and comparison between EnSR with SOO and without SOO

We have implemented satellite data assimilation combined with SOO. However, this does not mean in terms of methodology, ensemble-based data assimilation without SOO cannot work. Under that circumstance, applying data assimilation on 2D measurements and 3D concentrations, the operator  $H_k$  in Eq. (A5) does not select the grid cell in  $x(k)$ , but integrates all the vertical grid cells to calculate 2D mass loadings. This approach (denoted EnSR without SOO) would simplify the assimilation by only using 2D mass loadings. Although we focused SOO as a new way (as introduced in the introduction) to deal with satellite 3D data assimilation, the assimilation effects between with and without SOO should be better compared/studied in order to determine whether SOO is an effective approach.

Comparing to the EnSR implementations with SOO in Fig. 5c/ Fig. 6c, the cases of EnSR without SOO are shown in Fig. 5d/ Fig. 6d. Taking the SEVIRI retrieved mass loadings (Fig. 5a/ Fig. 6a) as references, it is revealed that EnSR without SOO performs better than the case without assimilation (Fig. 5b/ Fig. 6b), but worse than EnSR with SOO. One may also want to check the assimilation effect without SOO at the initial analysis time (i.e., 01:00 UTC, 16 May 2010), which is illustrated in Fig. 7. It can be seen that the assimilation difference between with and without SOO is small (by comparing Fig. 7c and 7d). While, at the second analysis time (i.e., 02:00 UTC, 16 May 2010) the results show much bigger differences (between Fig. 7g and Fig. 7h). These results verify and examine the influences of the artificial/spurious vertical correlations (caused by the integral-type of  $H_k$ , see introduction). These influences are examined to be accumulated step by step in our volcanic ash application and must be considered/avoided with respect to an acceptable assimilation result.

Now it is explained for our application why we chose SOO to compare measurements and model results in the model space rather than in the measurement space. Although the complications would be avoided if we do the analysis step in measurement space, however, the assimilation accuracy will then be worse than the case in the 3D model space by using SOO. Note that we perform EnSR without SOO in a standard/general way. We expect the problem of artificial vertical correlations (for volcanic ash plumes) may be partially compensated by employing some diagnostic or correction approaches, as discussed in (Blayo et al., 2014; Houtekamer and Zhang, 2016) for other applications. However, this would add many complications/difficulties to standard EnSR assimilation and whether/how it would work remains unknown (at the moment, no literature has reported on this issue for our application), and that it would be another research.

In this study, we focus on a way not dealing with the artificial vertical correlations, and we propose SOO by incorporating data and information available. The additional data (e.g., cloud top height and thickness information) are important for SOO, which describes the structure of a volcanic ash plume; we also provide an idea in the sense of incorporating many available measurements. In addition, we expect the SOO can be potentially improved by incorporating more data, but at the moment DA with SOO has shown its advantage than the standard way (without SOO) in dealing with passive satellite data assimilation.

## 6 Evaluation of the effective forecast duration after satellite data assimilation for the distal part of the Eyjafjallajökull volcano

According to Section 4.3, the accuracy of volcanic ash state is significantly improved by ensemble-based data assimilation after a continuous assimilation period (e.g., two days). Apparently, with the improved state as initialization, an improved forecast can be obtained (Fu et al., 2015). However, it remains unknown how long the improvement on forecasts will last.

To investigate the effective duration of the improved ash forecasts after assimilation, a one-day forecast is performed by initializing EnSR analyzed state (Fig. 6c) at 00:00 UTC 18 May 2010. Fig. 8 shows the forecast results after assimilation (first column in Fig. 8), the SEVIRI retrieved measurements (second column in Fig. 8) and the forecast results without assimilation (third column in Fig. 8). Without loss of generality, 06:00, 12:00 and 18:00 UTC are chosen to evaluate the comparisons over three divided distal regions of interest (denoted R1–R3). Note that we do not evaluate the near-volcano region (i.e., the left part of R1 in Fig. 8a), where the improved forecasts can be quickly influenced by the continuously noisy emissions. Thus it is safe to take the effective forecast duration for the near-volcano region as "zero hour".

For the region R1, the improved forecast after assimilation can last for 6 hours. This is viewed by that at 06:00 UTC, the forecast after assimilation (see R1 in Fig. 8a) is closer to the measurements (R1 in Fig. 8b) than the forecast without assimilation (R1 in Fig. 8c). However, the improvement diminishes after 6 hours (see the second and third rows in Fig. 8).

For the region R2, the forecast after DA at 06:00/12:00 UTC (R2 in Fig. 8a/ 8d) has a good match with the retrieved mass loadings (R2 in Fig. 8b/ 8e). However, we are not sure whether the good match remains at the time 18:00 UTC, because there seems to be lack of data at that time (see R2 in Fig. 8h). Therefore, it is better to evaluate the effective forecast duration after DA with SOO for R2 is 12 hours.

For the region R3, at the three times 06:00/12:00/18:00 UTC, the forecasts after DA are generally better than forecasts without DA by comparing with the measurements. However it should be noted that in Fig. 8e, some higher values (over  $3.5 \text{ g m}^{-2}$ ) are indeed retrieved in R3, but not in the forecasts after DA.

Our initial experimental tests show that, the effective time durations of the forecasts after satellite data assimilation with SOO can be considered as 6 hours for the region R1, 12 hours for the region R2, and 18 hours for the region R3. It also shows to us that the effective forecast duration tends to be longer as the region is farther away from the volcano. This is because longer time is needed for the influences of inaccurate ESPs to reach the areas farther from the volcano.

These results are evaluated using satellite retrieved data. For a further test, we employ another type of independent data. For this purpose, we use aircraft-based measurements (see details in Appendix B). Fig. 9a shows the flight route of the aircraft (in the region R3). Fig. 9b and 9c are the comparison of aircraft  $\text{PM}_{10}$  measurements against the forecasted concentrations after assimilation and without assimilation. Note that the low magnitude of aircraft measurements may result in little importance to verify high ash concentrations, but comparisons using them can indicate how good the assimilation is at reconstructing the outskirts/boundaries of the ash plume, which is important to describe the plume's structure.

For the period from 09:30 to 11:00 UTC (Fig. 9b), although the forecasting time has been over 9 hours (i.e., the last assimilation is 9 hours ago), the forecasted concentrations still have a good match with the accurate aircraft measurements,

while the conventional forecast (i.e., forecast without assimilation) doesn't. This result shows the forecast over 11 hours after assimilation has also kept a high accuracy compared to the measurements. The result can be extended to 15 hours comparing with the other period from 12:30 to 15:00 UTC (Fig. 9c). This test result using independent aircraft data confirms our evaluation result using satellite data that for the region R3, the effective forecast duration after DA is about 18 hours.

5 Based on all of the above evaluations and in the view of the whole distal regions of interest (R1+R2+R3), 6 hours can be taken as the a reasonable effective time duration (after assimilation with SOO) for the case study. This time duration can be taken as an indication about how long a valid regional aviation advice based on the forecast after assimilation can last. It should be noted that for other cases (e.g., another volcanic eruption), the effective duration is different because it depends on the specific weather condition and the specific model used for forecasting. Thus, the effective duration for other case studies  
10 should be re-evaluated, and what we presented in this section can be useful for the readers to test it.

## 7 Conclusions

In this paper, we choose the Eyjafjallajökull volcanic ash plume in May 2010 as the study case. In this study, a Satellite Observational Operator (SOO) was developed to translate 2D satellite ash mass loadings to 3D ash concentrations. To extract ash concentrations, not only the SEVIRI data of ash mass loadings, ash cloud top height are employed, but also a reasonable  
15 assumption of the ash cloud thickness range (0.2–3 km), at the corresponding horizontal location of the SEVIRI retrieved measurements, are combined. One advantage of SOO is that it can use rough thickness information to get uncertain concentrations, which are suitable for the data assimilation methodology.

The extracted ash concentration measurements enable us to perform ensemble-based data assimilation in a 3D volcanic ash transport model. By employing a preprocessing procedure before data assimilation to generate new measurement values  
20 by averaging all surrounding measurements, the model representation error is approximately zero. The SOO error is also calculated, and the total measurement error (defined as the sum of the SOO error and the model representation error) is therefore quantified, which together with the concentrations describe the 3D measurements (mean, error) for a data assimilation system. The results showed the assimilation with SOO significantly reduces the estimation level of the conventional simulation. The accuracy of the volcanic ash state was shown to be significantly improved by the assimilation of satellite mass loadings.

25 In this study, we proposed SOO as a new manner in dealing with passive satellite data assimilation. The assimilation with SOO was verified and examined to be more advantageous than the standard assimilation which introduces severe artificial vertical correlations in volcanic ash application. The development of SOO provides an idea of incorporating data and information available together to provide more accurate volcanic ash forecasts.

With the improved volcanic ash state as initialization, improved volcanic ash forecasts are obtained. Evaluations using both  
30 satellite retrieved data and aircraft in situ measurements showed that the effective forecast time duration after satellite data assimilation with SOO is about 6 hours for the distal part of the Eyjafjallajökull volcanic eruption. The results also showed that the effective forecast duration (after DA with SOO) tends to be longer as the region is farther away from the volcano, which is because inaccurate ESPs require longer time to impact on the regions farther from the volcano. Note that for other cases

(e.g., other volcano), this duration should be different and should be re-evaluated due to its dependence on the specific weather condition and on the specific model.

In this study, we developed SOO by considering cases where one singular ash cloud is present. Actually, it could happen that there are several isolated volcanic ash clouds in the vertical direction. The methodology of SOO is also valid for these cases, where the top isolated ash cloud does not correspond to the full but to a fraction of SEVIRI ash mass loadings. In this study, two of the Eruption Source Parameters (ESPs)–Plume Height (PH) and Mass Eruption Rate (MER) are made uncertain to generate DA ensembles. Actually the uncertainties can also be added in other ESPs, e.g., Vertical Mass Distribution (VMD) and Particle Size Distribution (PSD). However, adding noise in VMD and PSD should be very careful to keep their empirical/realistic distribution, e.g., “umbrella” shaped VMD (Sparks et al., 1997) and PSD for different types of eruption (Durant and Rose, 2009). Otherwise, the noisy VMD or PSD could provide unphysically biased prior ensemble plumes, resulting in DA algorithm impossible to reconstruct physical plume estimates. In this paper, we applied an off-line approach for model running and simply used the deterministic meteorological input data. Actually these data also contain uncertainties which have an influence on ash cloud transport. In future work, for more accurate ash forecasting, uncertainties in the meteorological data like wind speed should also be taken into account.

Recently, a large number of national weather services has implemented ceilometer networks, mainly for monitoring the dispersion of volcanic ash clouds (Wiegner et al., 2014). These data set will be (and in part are already) available in near real time and will provide information about the (horizontal and) vertical distribution (with some restrictions due to cloud cover; but this is also true for space borne observations). Thus, they could be promising candidates for data assimilation as well, but there are indeed some caveats. It will be interesting for future research to make use of and demonstrate the case for using ground-based lidars.

## 8 Data availability

All the satellite data shown in Fig. 1 are available and can be downloaded from [http://vast.nilu.no/test-database/volcano/Eyjafjallajokull/eruption/2010-04-14/main\\_data\\_type/Satellite/specific\\_data\\_type/seviri/](http://vast.nilu.no/test-database/volcano/Eyjafjallajokull/eruption/2010-04-14/main_data_type/Satellite/specific_data_type/seviri/) (Registration required). The aircraft data used in this study are available from Fig. 9b, c. The model output data can be accessed by request (G.Fu@tudelft.nl).

## 25 Appendix A: The ensemble square root filter

The ensemble square root filter (EnSR) is essentially a Monte Carlo sequential method (Evensen, 2003), based on the representation of the probability density of the state estimate by an ensemble of  $N$  states,  $\xi_1, \xi_2, \dots, \xi_N$ . Each ensemble member is assumed as one sample of a true state distribution. The required ensemble size depends on the model’s nonlinearity and the the involved uncertainties. For the application of the filter algorithm to a volcanic ash transport model, an ensemble size of 50 is considered acceptable for maintaining a balance between accuracy and computational cost (Fu et al., 2015, 2016). In the first step of this algorithm an ensemble of  $N$  volcanic ash state  $\xi^a(0)$  is generated to represent the uncertainty in the initial

condition  $\mathbf{x}(0)$ . In the second step (the forecast step), the model propagates the ensemble members from time  $t_{k-1}$  to  $t_k$ :

$$\xi_j^f(k) = M_{k-1}(\xi_j^a(k-1)). \quad (\text{A1})$$

The state-space operator  $M_{k-1}$  describes the time evolution from the time  $t_{k-1}$  to  $t_k$  of the state vector which contains the ash concentrations in all the model grid boxes. The filter state at time  $t_k$  is a stochastic distribution with mean  $\mathbf{x}^f$  and covariance

5  $\mathbf{P}^f$  given by:

$$\mathbf{x}^f = \frac{1}{N} \left[ \sum_{j=1}^N \xi_j^f \right] \quad , \quad (\text{A2})$$

$$\mathbf{L}^f = [\xi_1^f - \mathbf{x}^f, \dots, \xi_N^f - \mathbf{x}^f] \quad , \quad (\text{A3})$$

$$\mathbf{P}^f = \frac{1}{N-1} [\mathbf{L}^f (\mathbf{L}^f)'] \quad , \quad (\text{A4})$$

The observational network at time  $t_k$  is defined by the observation operator  $H$  that maps state vector  $\mathbf{x}$  to observation space  $\mathbf{y}$

10 by

$$\mathbf{y}(k) = H_k(\mathbf{x}(k)) + \mathbf{v}(k), \quad (\text{A5})$$

where the observation error  $\mathbf{v}$  is drawn from Gaussian distribution with zero mean and covariance matrix  $\mathbf{R}$ . Here,  $\mathbf{y}$  contains the measurements of ash concentrations and  $\mathbf{R}$  is assumed to be a diagonal matrix with the square of the standard deviation (measurement uncertainty) as diagonal entries. The operator  $H$  selects the grid cell in  $\mathbf{x}(k)$  that corresponds to the observation

15 location. When measurements become available, the ensemble members are updated in the analysis step using the Kalman gain and their ensemble covariance matrix following:

$$\mathbf{K} = \mathbf{P}^f \mathbf{H}' [\mathbf{H} \mathbf{P}^f \mathbf{H}' + \mathbf{R}]^{-1} \quad , \quad (\text{A6})$$

$$\xi_j^a = \xi_j^f + \mathbf{K} [\mathbf{y} - \mathbf{H} \xi_j^f + \mathbf{v}_j] \quad , \quad (\text{A7})$$

$$\mathbf{P}^a = (\mathbf{I} - \mathbf{K} \mathbf{H}) \mathbf{P}^f \quad , \quad (\text{A8})$$

20 where  $\mathbf{v}_j$  represents realizations of the observation error  $v$ . To reduce the sampling errors introduced by adding random numbers  $\mathbf{v}_j$  to the observations, the analysis step can be written in a square root form (Evensen, 2004; Sakov and Oke, 2008a, b). Using the notations  $\mathbf{Y} = \mathbf{H} \mathbf{L}^f$  and  $\mathbf{S} = \mathbf{Y} \mathbf{Y}' + \mathbf{R}$ , the updated covariance matrix becomes:

$$\mathbf{P}^a = \mathbf{L}^a (\mathbf{L}^a)' = \mathbf{L}^f (\mathbf{I} - \mathbf{Y}' \mathbf{S}^{-1} \mathbf{Y}) (\mathbf{L}^f)' = \mathbf{L}^f \mathbf{T} \mathbf{T}' (\mathbf{L}^f)' \quad , \quad (\text{A9})$$

thus  $\mathbf{L}^a$  can be represented by

$$25 \quad \mathbf{L}^a = \mathbf{L}^f \mathbf{T} \quad , \quad (\text{A10})$$

where  $\mathbf{T}$  is an  $N \times N$  matrix which satisfies:  $\mathbf{T} \mathbf{T}' = \mathbf{I} - \mathbf{Y}' \mathbf{S}^{-1} \mathbf{Y}$ . It can be easily shown that there is a unique symmetric positive definite solution defined as the square root of the symmetric positive definite matrix:  $\mathbf{T}^s = [\mathbf{I} - \mathbf{Y}' \mathbf{S}^{-1} \mathbf{Y}]^{\frac{1}{2}}$ . By using



the eigenvalue decomposition, the matrix  $\mathbf{T}^s$  has the following form:

$$\mathbf{T}^s = \mathbf{C}\mathbf{\Lambda}^{\frac{1}{2}}\mathbf{C}', \quad (\text{A11})$$

where  $\mathbf{T}^s$  is referred as the symmetric factor. The symmetric algorithm defined above introduces the smallest analysis increments for an arbitrary compatible norm. The good performance of EnSR has been obtained on improving the forecast accuracies without introducing additional sampling errors (Evensen, 2004; Sakov and Oke, 2008a).

## Appendix B: Aircraft in situ measurements

Aircraft-based measurements allow sampling of the ash cloud with a high spatial and temporal resolution and by using optical particle counters (OPC) this type of measurement is estimated with a high accuracy of 10% (Weber et al., 2010).

In this study, the available aircraft measurements on 18 May 2010 from 09:30 to 15:30 UTC were used. The measurements were performed by the group Environmental Measurement Techniques at Düsseldorf university of Applied Sciences. The measurements took place in the North-West part of Germany including the border between the Netherlands and Germany, see Fig. 9a. The aircraft took off from the airfield “Schwarze Heide” in the Northern part of the Rhein-Ruhr area, headed along the Dutch-German border in the direction of the North Sea, continued towards Hamburg and then returned to the airfield. Along the route, concentrations of  $\text{PM}_{10}$  and  $\text{PM}_{2.5}$  were measured.

Note that the aircraft measurements represent  $\text{PM}_{10}$  concentration at inlet position while the model gives values which are averages of the concentration for a  $0.25^\circ \times 0.125^\circ \times 1$  km grid box. Assuming the uniformity of the fields, it is appropriate to compare these two values given that the measurements are made at different resolutions and by different methods. However, when the heterogeneity is a serious issue, the model representation error should also be better considered.

*Author contributions.* All authors participated in the design of the experiment and the analysis of the assimilation results. Guangliang Fu, Arjo Segers and Sha Lu modeled the volcanic ash transport using the LOTOS-EUROS. Guangliang Fu and Fred Prata validated SEVIRI measurements and provided them for the development of SSO. Guangliang Fu, Hai Xiang Lin, Arnold Heemink, and Fred Prata carried out data assimilation experiment, analyzed the results and finalized the paper.

*Acknowledgements.* We are very grateful to the editor and reviewers for their reviews and insightful comments. We thank the European Space Agency (ESA) project – Volcanic Ash Strategic initiative Team (VAST) for providing the satellite data for the 2010 Eyjafjallajökull volcanic eruption. We thank Prof. Konradin Weber (University of Applied Sciences, Environmental Measurement Techniques, Düsseldorf, Germany) for providing the real-time aircraft in situ measurements. We thank Dr. Arve Kylling at NILU-Norwegian Institute for Air Research for his kind assistance with interpretations of volcanic ash cloud height. In this paper, we perform the ensemble-based data assimilation using OpenDA (open source software, www.openda.com). The first and the last author thank the China Scholarship Council for the financial support to this research. We would also like to thank the Netherlands Supercomputing Centre (SURFsara) for providing us the computing facility: the Cartesius cluster.

## References

- Ansmann, A., Tesche, M., Groß, S., Freudenthaler, V., Seifert, P., Hiebsch, A., Schmidt, J., Wandinger, U., Mattis, I., Müller, D., and Wiegner, M.: The 16 April 2010 major volcanic ash plume over central Europe: EARLINET lidar and AERONET photometer observations at Leipzig and Munich, Germany, *Geophys. Res. Lett.*, 37, L13 810+, doi:10.1029/2010gl043809, 2010.
- 5 Blayo, E., Bocquet, M., Cosme, E., and Cugliandolo, L. F., eds.: *Advanced Data Assimilation for Geosciences*, Oxford University Press, doi:10.1093/acprof:oso/9780198723844.001.0001, 2014.
- Bocquet, M., Elbern, H., Eskes, H., Hirtl, M., Žabkar, R., Carmichael, G. R., Flemming, J., Inness, A., Pagowski, M., Pérez Camaño, J. L., Saide, P. E., San Jose, R., Sofiev, M., Vira, J., Baklanov, A., Carnevale, C., Grell, G., and Seigneur, C.: Data assimilation in atmospheric chemistry models: current status and future prospects for coupled chemistry meteorology models, *Atmospheric Chemistry and Physics*, 15, 5325–5358, doi:10.5194/acp-15-5325-2015, 2015.
- 10 Bonadonna, C. and Costa, A.: Plume height, volume, and classification of explosive volcanic eruptions based on the Weibull function, 75, 1–19, doi:10.1007/s00445-013-0742-1, 2013.
- Casadevall, T. J.: The 1989–1990 eruption of Redoubt Volcano, Alaska: impacts on aircraft operations, *Journal of Volcanology and Geothermal Research*, 62, 301–316, doi:10.1016/0377-0273(94)90038-8, 1994.
- 15 Corradini, S., Spinetti, C., Carboni, E., Tirelli, C., Buongiorno, M. F., Pugnani, S., and Gangale, G.: Mt. Etna tropospheric ash retrieval and sensitivity analysis using moderate resolution imaging spectroradiometer measurements, *Journal of Applied Remote Sensing*, 2, 023 550–023 550–20, doi:10.1117/1.3046674, 2008.
- Dacre, H. F., Grant, A. L. M., Harvey, N. J., Thomson, D. J., Webster, H. N., and Marenco, F.: Volcanic ash layer depth: Processes and mechanisms, *Geophys. Res. Lett.*, 42, 2014GL062 454+, doi:10.1002/2014gl062454, 2015.
- 20 de Laat, A. T. J. and van der A, R. J.: Validation and evaluation of SEVIRI volcanic ash heights, Tech. rep., Royal Netherlands Meteorological Institute (KNMI), <http://bibliotheek.knmi.nl/knmipubTR/TR337.pdf>, 2012.
- Draxler, R. R. and Hess, G. D.: An overview of the HYSPLIT\_4 modelling system for trajectories, dispersion, and deposition, *Australian Meteorological Magazine*, 47, 295–308, <http://www.arl.noaa.gov/documents/reports/MetMag.pdf>, 1998.
- Durant, A. J. and Rose, W. I.: Sedimentological constraints on hydrometeor-enhanced particle deposition: 1992 Eruptions of Crater Peak, Alaska, *Journal of Volcanology and Geothermal Research*, 186, 40–59, doi:10.1016/j.jvolgeores.2009.02.004, 2009.
- 25 EASA: EASA Safety Information Bulletin 2010-17R7, <http://ad.easa.europa.eu/ad/2010-17R7>, 2015.
- Eliasson, J., Palsson, A., and Weber, K.: Monitoring ash clouds for aviation, *Nature*, 475, 455, doi:10.1038/475455b, 2011.
- Emeis, S., Forkel, R., Junkermann, W., Schäfer, K., Flentje, H., Gilge, S., Fricke, W., Wiegner, M., Freudenthaler, V., Groß, S., Ries, L., Meinhardt, F., Birmili, W., Münkler, C., Obleitner, F., and Suppan, P.: Measurement and simulation of the 16/17 April 2010 Eyjafjallajökull volcanic ash layer dispersion in the northern Alpine region, *Atmospheric Chemistry and Physics*, 11, 2689–2701, doi:10.5194/acp-11-2689-2011, 2011.
- 30 Evensen, G.: Sequential data assimilation with a nonlinear quasi-geostrophic model using Monte Carlo methods to forecast error statistics, *J. Geophys. Res.*, 99, 10 143–10 162, doi:10.1029/94jc00572, 1994.
- Evensen, G.: The Ensemble Kalman Filter: theoretical formulation and practical implementation, *Ocean Dynamics*, 53, 343–367, doi:10.1007/s10236-003-0036-9, 2003.
- 35 Evensen, G.: Sampling strategies and square root analysis schemes for the EnKF, *Ocean Dynamics*, 54, 539–560, doi:10.1007/s10236-004-0099-2, 2004.

- Evensen, G. and van Leeuwen, P. J.: An Ensemble Kalman Smoother for Nonlinear Dynamics, *Mon. Wea. Rev.*, 128, 1852–1867, doi:10.1175/1520-0493(2000)128%3C1852:aeksfn%3E2.0.co;2, 2000.
- Flentje, H., Claude, H., Elste, T., Gilge, S., Köhler, U., Plass-Dülmer, C., Steinbrecht, W., Thomas, W., Werner, A., and Fricke, W.: The Eyjafjallajökull eruption in April 2010 &ndash; detection of volcanic plume using in-situ measurements, ozone sondes and a new generation  
5 ceilometer network, *Atmospheric Chemistry and Physics Discussions*, 10, 14 947–14 968, doi:10.5194/acpd-10-14947-2010, 2010.
- Francis, P. N., Cooke, M. C., and Saunders, R. W.: Retrieval of physical properties of volcanic ash using Meteosat: A case study from the 2010 Eyjafjallajökull eruption, *J. Geophys. Res.*, 117, D00U09+, doi:10.1029/2011jd016788, 2012.
- Fu, G., Lin, H. X., Heemink, A. W., Segers, A. J., Lu, S., and Palsson, T.: Assimilating aircraft-based measurements to improve Forecast Accuracy of Volcanic Ash Transport, *Atmospheric Environment*, 115, 170–184, doi:10.1016/j.atmosenv.2015.05.061, 2015.
- 10 Fu, G., Heemink, A., Lu, S., Segers, A., Weber, K., and Lin, H.-X.: Model-based aviation advice on distal volcanic ash clouds by assimilating aircraft in situ measurements, *Atmospheric Chemistry and Physics*, 16, 9189–9200, doi:10.5194/acp-16-9189-2016, 2016.
- Gieske, A. S. M., Hendrikse, J., Retsios, V., van Leeuwen, B., Maathuis, B. H. P., Romaguera, M., Sobrino, J. A., Timmermans1, W. J., and Su1, Z.: Processing of MSG-1 SEVIRI data in the thermal infrared–Algorithm development with the use of the SPARC 2004 data set, in: *Proc. WPP-250: SPARC Final Workshop*, pp. 1–8, Enschede, Netherlands, [http://www.itc.nl/library/papers\\_2005/conf/gieske\\_pro.pdf](http://www.itc.nl/library/papers_2005/conf/gieske_pro.pdf),  
15 2005.
- Gudmundsson, M. T., Pedersen, R., Vogfjörd, K., Thorbjarnardóttir, B., Jakobsdóttir, S., and Roberts, M. J.: Eruptions of Eyjafjallajökull Volcano, Iceland, *Eos Trans. AGU*, 91, 190–191, doi:10.1029/2010eo210002, 2010.
- Houtekamer, P. L. and Zhang, F.: Review of the Ensemble Kalman Filter for Atmospheric Data Assimilation, *Mon. Wea. Rev.*, 144, 4489–4532, doi:10.1175/mwr-d-15-0440.1, 2016.
- 20 Jones, A., Thomson, D., Hort, M., and Devenish, B.: The U.K. Met Office’s Next-Generation Atmospheric Dispersion Model, NAME III, in: *Air Pollution Modeling and Its Application XVII*, edited by Borrego, C. and Norman, A.-L., pp. 580–589, Springer US, doi:10.1007/978-0-387-68854-1\_62, 2007.
- Kirkup, L. and Frenkel, R. B.: Introduction to uncertainty in measurement, chap. 4, pp. 35–52, Cambridge University Press, Cambridge, doi:10.1017/cbo9780511755538.006, 2006.
- 25 Kokkalis, P., Papayannis, A., Amiridis, V., Mamouri, R. E., Veselovskii, I., Kolgotin, A., Tsaknakis, G., Kristiansen, N. I., Stohl, A., and Mona, L.: Optical, microphysical, mass and geometrical properties of aged volcanic particles observed over Athens, Greece, during the Eyjafjallajökull eruption in April 2010 through synergy of Raman lidar and sunphotometer measurements, *Atmospheric Chemistry and Physics*, 13, 9303–9320, doi:10.5194/acp-13-9303-2013, 2013.
- Kylling, A., Kristiansen, N., Stohl, A., Buras-Schnell, R., Emde, C., and Gasteiger, J.: A model sensitivity study of the impact of clouds  
30 on satellite detection and retrieval of volcanic ash, *Atmospheric Measurement Techniques*, 8, 1935–1949, doi:10.5194/amt-8-1935-2015, 2015.
- Lu, S., Lin, H. X., Heemink, A., Segers, A., and Fu, G.: Estimation of volcanic ash emissions through assimilating satellite data and ground-based observations, *J. Geophys. Res. Atmos.*, 121, 10,971–10,994, doi:10.1002/2016JD025131, 2016a.
- Lu, S., Lin, H. X., Heemink, A. W., Fu, G., and Segers, A. J.: Estimation of Volcanic Ash Emissions Using Trajectory-Based 4D-Var Data  
35 Assimilation, *Mon. Wea. Rev.*, 144, 575–589, doi:10.1175/mwr-d-15-0194.1, 2016b.
- Marengo, F., Johnson, B., Turnbull, K., Newman, S., Haywood, J., Webster, H., and Ricketts, H.: Airborne lidar observations of the 2010 Eyjafjallajökull volcanic ash plume, *J. Geophys. Res.*, 116, D00U05+, doi:10.1029/2011jd016396, 2011.

- Mastin, L. G., Guffanti, M., Servranckx, R., Webley, P., Barsotti, S., Dean, K., Durant, A., Ewert, J. W., Neri, A., Rose, W. I., Schneider, D., Siebert, L., Stunder, B., Swanson, G., Tupper, A., Volentik, A., and Waythomas, C. F.: A multidisciplinary effort to assign realistic source parameters to models of volcanic ash-cloud transport and dispersion during eruptions, *Journal of Volcanology and Geothermal Research*, 186, 10–21, doi:10.1016/j.jvolgeores.2009.01.008, 2009.
- 5 Navas-Guzmán, F., Müller, D., Bravo-Aranda, J. A., Guerrero-Rascado, J. L., Granados-Muñoz, M. J., Pérez-Ramírez, D., Olmo, F. J., and Alados-Arboledas, L.: Eruption of the Eyjafjallajökull Volcano in spring 2010: Multiwavelength Raman lidar measurements of sulphate particles in the lower troposphere, *J. Geophys. Res. Atmos.*, 118, 1804–1813, doi:10.1002/jgrd.50116, 2013.
- Nemuc, A., Stachlewska, I., Vasilescu, J., Górska, A., Nicolae, D., and Talianu, C.: Optical properties of long-range transported volcanic ash over Romania and Poland during Eyjafjallajökull eruption in 2010, 62, 350–366, doi:10.2478/s11600-013-0180-7, 2014.
- 10 Oberhuber, J. M., Herzog, M., Graf, H.-F., and Schwanke, K.: Volcanic plume simulation on large scales, *Journal of Volcanology and Geothermal Research*, 87, 29–53, doi:10.1016/s0377-0273(98)00099-7, 1998.
- Oxford-Economics: The Economic Impacts of Air Travel Restrictions Due to Volcanic Ash, Report for Airbus, Tech. rep., <http://www.oxfordeconomics.com/my-oxford/projects/129051>, 2010.
- Pappalardo, G., Amodeo, A., Ansmann, A., Apituley, A., Alados Arboledas, L., Balis, D., Böckmann, C., Chaikovsky, A., Comeron, A., D’Amico, G., De Tomasi, F., Freudenthaler, V., Giannakaki, E., Giunta, A., Grigorov, I., Gustafsson, O., Gross, S., Haefelin, M., Iarlori, M., Kinne, S., Linné, H., Madonna, F., Mamouri, R., Mattis, I., McAuliffe, M., Molero, F., Mona, L., Müller, D., Mitev, V., Nicolae, D., Papayannis, A., Perrone, M. R., Pietruczuk, A., Pujadas, M., Putaud, J.-P., Ravetta, F., Rizi, V., Serikov, I., Sicard, M., Simeonov, V., Spinelli, N., Stebel, K., Trickl, T., Wandinger, U., Wang, X., Wagner, F., and Wiegner, M.: EARLINET observations of the Eyjafjallajökull ash plume over Europe, vol. 7832, pp. 78 320J–78 320J–9, doi:10.1117/12.869016, 2010.
- 15 Pappalardo, G., Mona, L., D’Amico, G., Wandinger, U., Adam, M., Amodeo, A., Ansmann, A., Apituley, A., Alados Arboledas, L., Balis, D., Boselli, A., Bravo-Aranda, J. A., Chaikovsky, A., Comeron, A., Cuesta, J., De Tomasi, F., Freudenthaler, V., Gausa, M., Giannakaki, E., Giehl, H., Giunta, A., Grigorov, I., Groß, S., Haefelin, M., Hiebsch, A., Iarlori, M., Lange, D., Linné, H., Madonna, F., Mattis, I., Mamouri, R. E., McAuliffe, M. A. P., Mitev, V., Molero, F., Navas-Guzman, F., Nicolae, D., Papayannis, A., Perrone, M. R., Pietras, C., Pietruczuk, A., Pisani, G., Preißler, J., Pujadas, M., Rizi, V., Ruth, A. A., Schmidt, J., Schnell, F., Seifert, P., Serikov, I., Sicard, M., Simeonov, V., Spinelli, N., Stebel, K., Tesche, M., Trickl, T., Wang, X., Wagner, F., Wiegner, M., and Wilson, K. M.: Four-dimensional distribution of the 2010 Eyjafjallajökull volcanic cloud over Europe observed by EARLINET, *Atmospheric Chemistry and Physics*, 13, 4429–4450, doi:10.5194/acp-13-4429-2013, 2013.
- 20 Prata, A. J.: Infrared radiative transfer calculations for volcanic ash clouds, *Geophys. Res. Lett.*, 16, 1293–1296, doi:10.1029/gl016i01p01293, 1989.
- 30 Prata, A. J. and Prata, A. T.: Eyjafjallajökull volcanic ash concentrations determined using Spin Enhanced Visible and Infrared Imager measurements, *Journal of Geophysical Research: Atmospheres*, 117, n/a, doi:10.1029/2011jd016800, 2012.
- Prata, A. T., Siems, S. T., and Manton, M. J.: Quantification of volcanic cloud top heights and thicknesses using A-train observations for the 2008 Chaitén eruption, *J. Geophys. Res. Atmos.*, 120, 2014JD022 399+, doi:10.1002/2014jd022399, 2015.
- Sakov, P. and Oke, P. R.: A deterministic formulation of the ensemble Kalman filter: an alternative to ensemble square root filters, *Tellus A*, 35, 361–371, doi:10.1111/j.1600-0870.2007.00299.x, 2008a.
- Sakov, P. and Oke, P. R.: Implications of the Form of the Ensemble Transformation in the Ensemble Square Root Filters, *Mon. Wea. Rev.*, 136, 1042–1053, doi:10.1175/2007mwr2021.1, 2008b.

- Schaap, M., Timmermans, R. M. A., Roemer, M., Boersen, G. A. C., Bultjes, P. J. H., Sauter, F. J., Velders, G. J. M., and Beck, J. P.: The LOTOS EUROS model: description, validation and latest developments, *International Journal of Environment and Pollution*, 32, 270+, doi:10.1504/ijep.2008.017106, 2008.
- Schäfer, K., Thomas, W., Peters, A., Ries, L., Obleitner, F., Schnelle-Kreis, J., Birmili, W., Diemer, J., Fricke, W., Junkermann, W., Pitz, M., Emeis, S., Forkel, R., Suppan, P., Flentje, H., Gilge, S., Wichmann, H. E., Meinhardt, F., Zimmermann, R., Weinhold, K., Soentgen, J., Münkler, C., Freuer, C., and Cyrys, J.: Influences of the 2010 Eyjafjallajökull volcanic plume on air quality in the northern Alpine region, *Atmospheric Chemistry and Physics*, 11, 8555–8575, doi:10.5194/acp-11-8555-2011, 2011.
- Schmetz, J., Pili, P., Tjemkes, S., Just, D., Kerkmann, J., Rota, S., and Ratier, A.: An Introduction to Meteosat Second Generation (MSG), *Bull. Amer. Meteor. Soc.*, 83, 977–992, doi:10.1175/1520-0477(2002)083%3C0977:aitmsg%3E2.3.co;2, 2002.
- Schumann, U., Weinzierl, B., Reitebuch, O., Schlager, H., Minikin, A., Forster, C., Baumann, R., Sailer, T., Graf, K., Mannstein, H., Voigt, C., Rahm, S., Simmet, R., Scheibe, M., Lichtenstern, M., Stock, P., Rüba, H., Schäuble, D., Tafferner, A., Rautenhaus, M., Gerz, T., Ziereis, H., Krautstrunk, M., Mallaun, C., Gayet, J. F., Lieke, K., Kandler, K., Ebert, M., Weinbruch, S., Stohl, A., Gasteiger, J., Groß, S., Freudenthaler, V., Wiegner, M., Ansmann, A., Tesche, M., Olafsson, H., and Sturm, K.: Airborne observations of the Eyjafjalla volcano ash cloud over Europe during air space closure in April and May 2010, *Atmospheric Chemistry and Physics*, 11, 2245–2279, doi:10.5194/acp-11-2245-2011, 2011.
- Searcy, C., Dean, K., and Stringer, W.: PUFF: A high-resolution volcanic ash tracking model, *Journal of Volcanology and Geothermal Research*, 80, 1–16, doi:10.1016/s0377-0273(97)00037-1, 1998.
- Sparks, R. S. J., Burski, M. I., Carey, S. N., Gilbert, J. S., Glaze, L. S., Sigurdsson, H., and Woods, A. W.: *Volcanic Plumes*, Wiley, 1 edn., <http://www.worldcat.org/isbn/0471939013>, 1997.
- Stohl, A., Prata, A. J., Eckhardt, S., Clarisse, L., Durant, A., Henne, S., Kristiansen, N. I., Minikin, A., Schumann, U., Seibert, P., Stebel, K., Thomas, H. E., Thorsteinsson, T., Tørseth, K., and Weinzierl, B.: Determination of time- and height-resolved volcanic ash emissions and their use for quantitative ash dispersion modeling: the 2010 Eyjafjallajökull eruption, *Atmospheric Chemistry and Physics*, 11, 4333–4351, doi:10.5194/acp-11-4333-2011, 2011.
- Verlaan, M. and Heemink, A. W.: Tidal flow forecasting using reduced rank square root filters, *Stochastic Hydrology and Hydraulics*, 11, 349–368, doi:10.1007/bf02427924, 1997.
- Weber, K., Vogel, A., Fischer, C., van Haren, G., and Pohl, T.: Airborne measurements of the Eyjafjallajökull volcanic ash plume over northwestern Germany with a light aircraft and an optical particle counter: first results, vol. 7832, pp. 78 320P–78 320P–15, doi:10.1117/12.869629, 2010.
- Weber, K., Eliasson, J., Vogel, A., Fischer, C., Pohl, T., van Haren, G., Meier, M., Grobéty, B., and Dahmann, D.: Airborne in-situ investigations of the Eyjafjallajökull volcanic ash plume on Iceland and over north-western Germany with light aircrafts and optical particle counters, *Atmospheric Environment*, 48, 9–21, doi:10.1016/j.atmosenv.2011.10.030, 2012.
- Webley, P. W., Steensen, T., Stuefer, M., Grell, G., Freitas, S., and Pavolonis, M.: Analyzing the Eyjafjallajökull 2010 eruption using satellite remote sensing, lidar and WRF-Chem dispersion and tracking model, *J. Geophys. Res.*, 117, D00U26+, doi:10.1029/2011jd016817, 2012.
- Wiegner, M., Gasteiger, J., Groß, S., Schnell, F., Freudenthaler, V., and Forkel, R.: Characterization of the Eyjafjallajökull ash-plume: Potential of lidar remote sensing, *Physics and Chemistry of the Earth, Parts A/B/C*, 45-46, 79–86, doi:10.1016/j.pce.2011.01.006, 2012.
- Wiegner, M., Madonna, F., Biniotoglou, I., Forkel, R., Gasteiger, J., Geiß, A., Pappalardo, G., Schäfer, K., and Thomas, W.: What is the benefit of ceilometers for aerosol remote sensing? An answer from EARLINET, *Atmospheric Measurement Techniques*, 7, 1979–1997, doi:10.5194/amt-7-1979-2014, 2014.

Winker, D. M., Liu, Z., Omar, A., Tackett, J., and Fairlie, D.: CALIOP observations of the transport of ash from the Eyjafjallajökull volcano in April 2010, *Journal of Geophysical Research: Atmospheres*, 117, n/a, doi:10.1029/2011jd016499, 2012.

Witham, C. S., Hort, M. C., Potts, R., Servranckx, R., Husson, P., and Bonnardot, F.: Comparison of VAAC atmospheric dispersion models using the 1 November 2004 Grimsvötn eruption, *Met. Apps*, 14, 27–38, doi:10.1002/met.3, 2007.

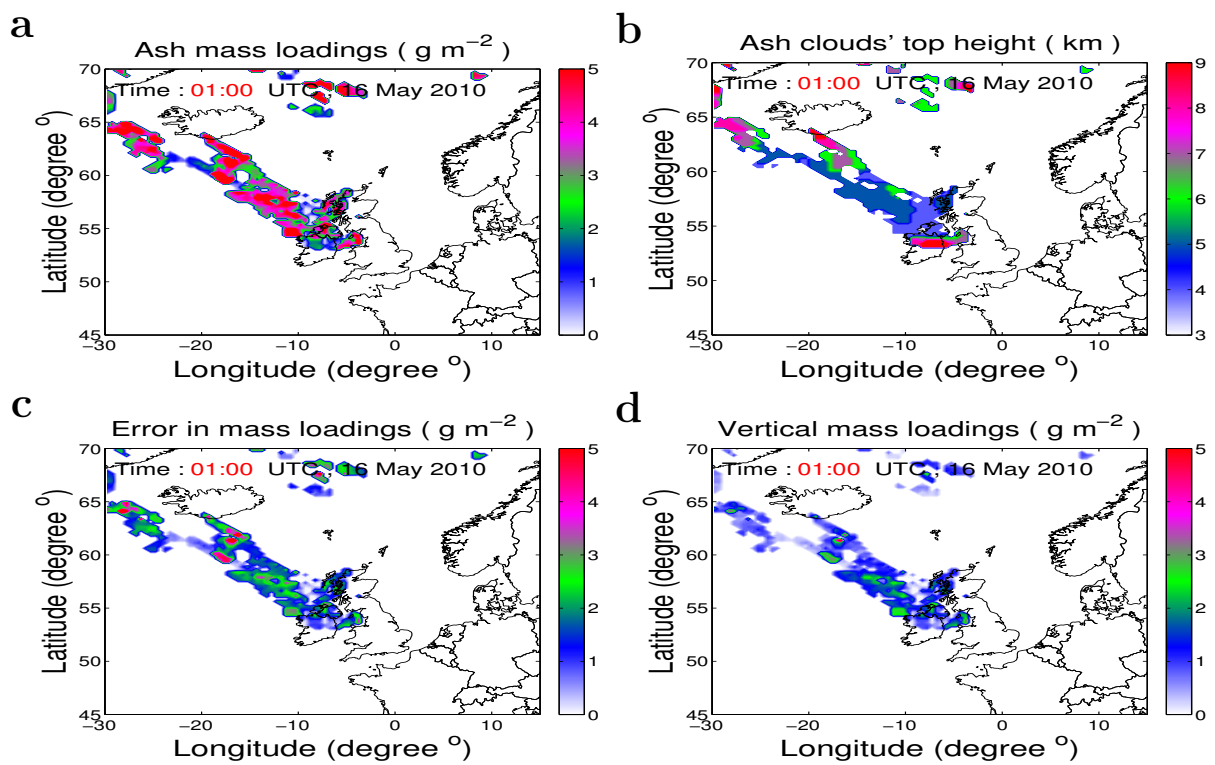


**Figure 1.** Available volcanic ash data from SEVIRI on 16 May 2010 at 01:00 UTC. Data are acquired from the European Space Agency (ESA) funded projects Volcanic Ash Strategic Initiative Team (VAST). **a**, Ash mass loadings. Values at 0 mean no data. **b**, Ash cloud top height. **c**, Error in the retrieved ash mass loadings **a**. **d**, Ash mass loadings in the vertical direction, i.e.,  $M_v$  in Eq. (1).

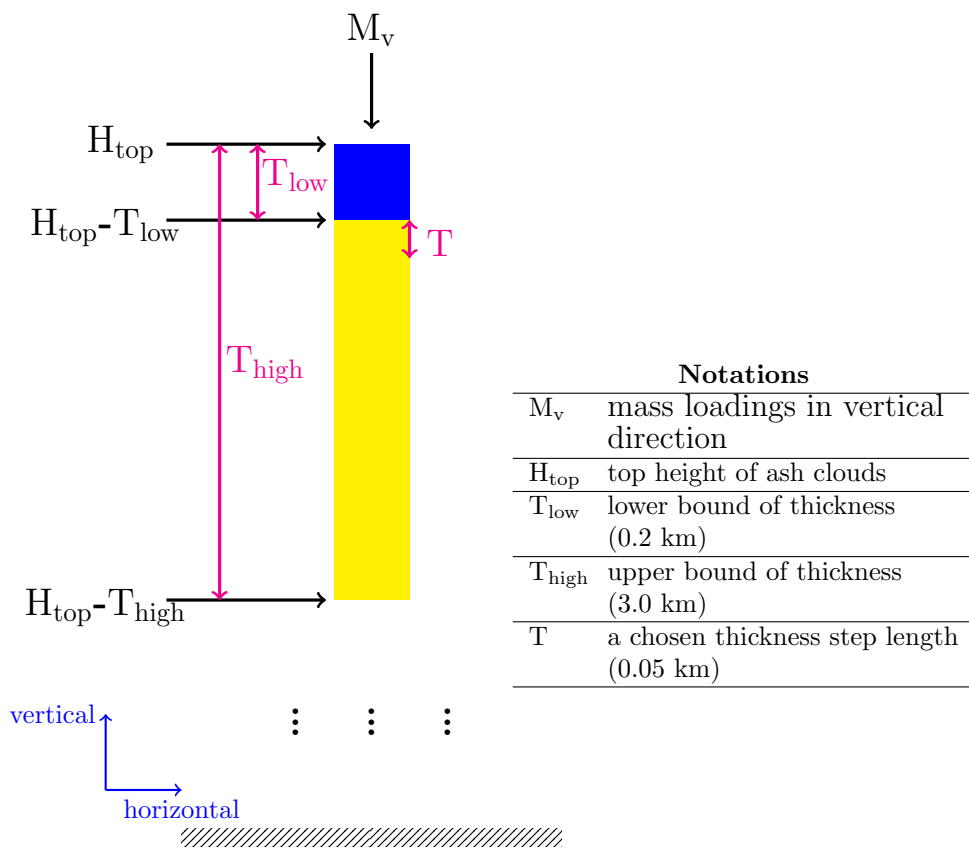


Figure 2. Illustration of the Satellite Observational Operator (SOO).



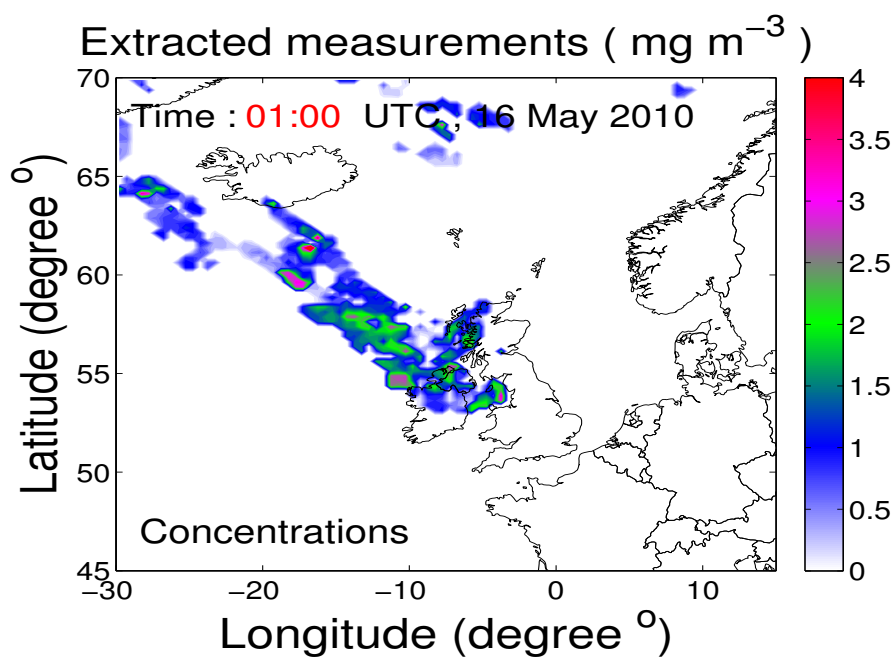
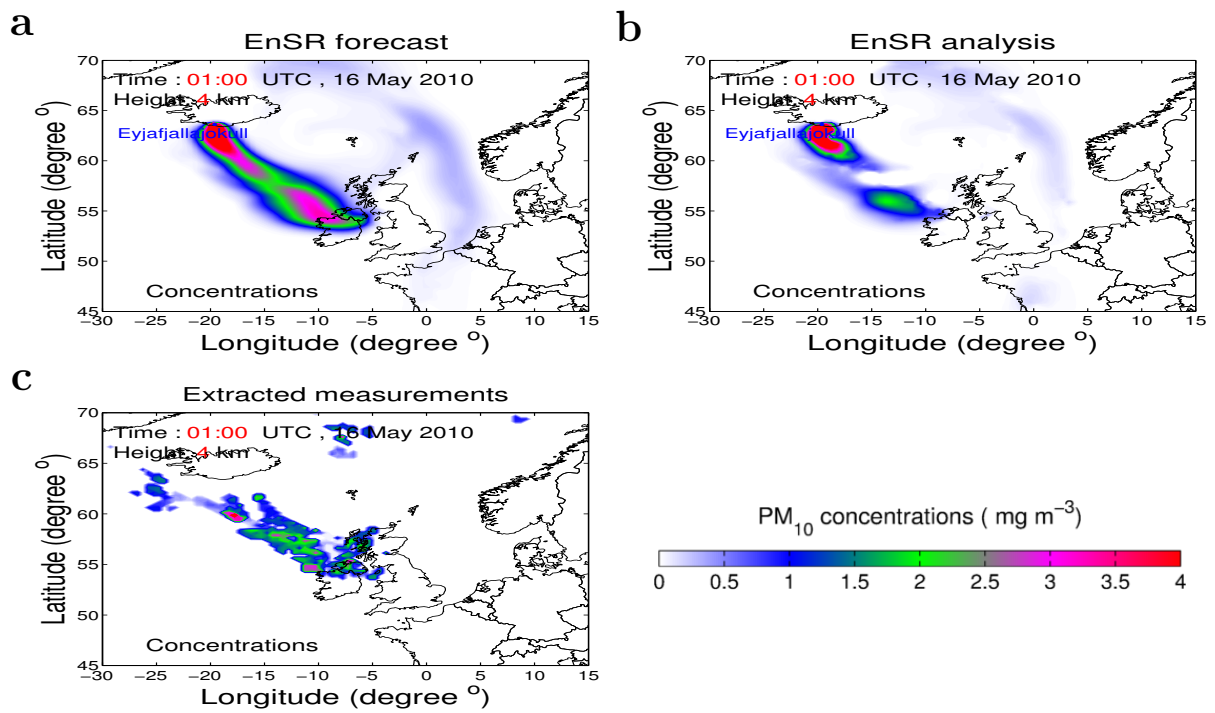
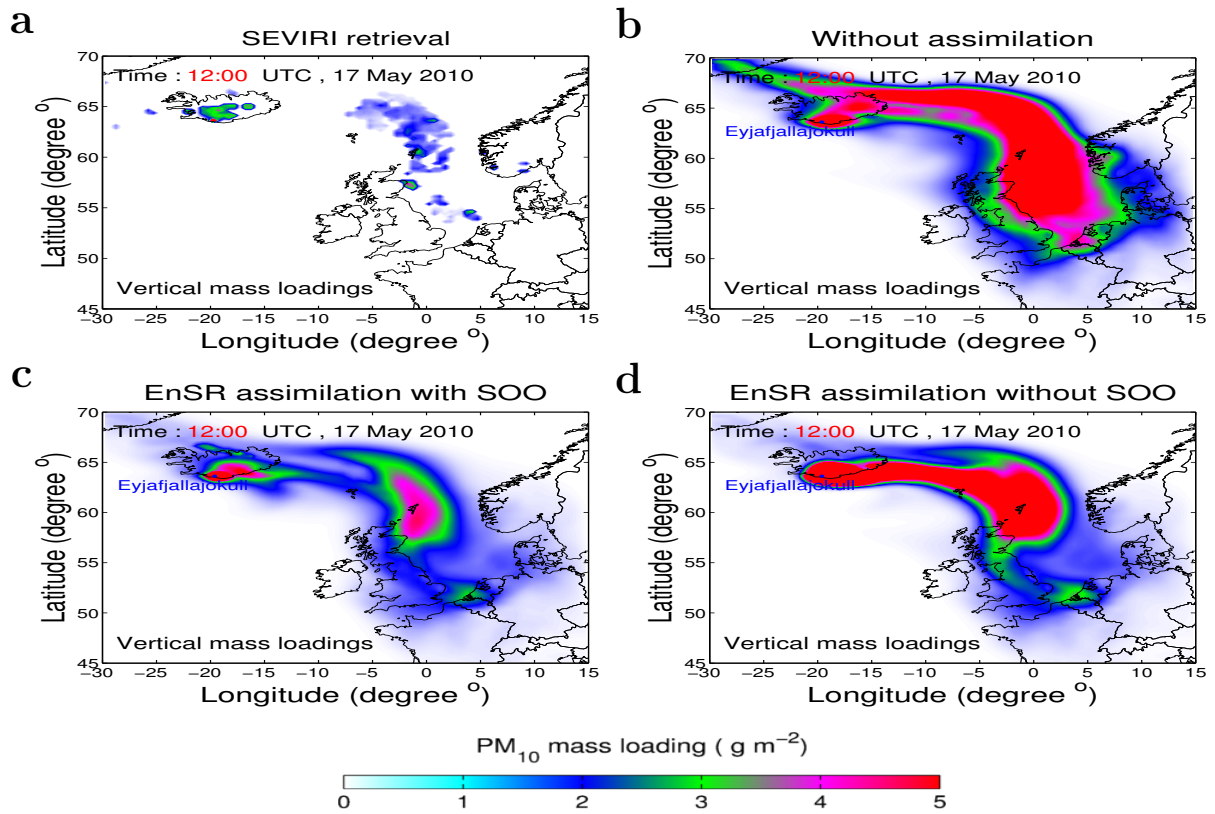


Figure 3. Extracted ash concentrations by the Satellite Observational Operator (at 16 May 2010 at 01:00 UTC).



**Figure 4.** Examination of EnSR effect when assimilating SEVIRI-extracted ash concentrations at 01:00 UTC 16 May 2010. **a**, EnSR forecast (ensemble mean) of PM<sub>10</sub> concentrations. **b**, EnSR analysis (ensemble mean) of PM<sub>10</sub> concentrations. **c**, Extracted measurements of PM<sub>10</sub> concentrations from the SOO. **a, b, c** are illustrated at a height of 4 km.



**Figure 5.**  $PM_{10}$  mass loadings with EnSR against the SEVIRI retrieval at 12:00 UTC 17 May 2010. **a**, SEVIRI retrieved mass loadings in the vertical direction, i.e.,  $M_v$  in Eq. (1). **b**, Simulated mass loadings without assimilation. **c**, Mass loadings (ensemble mean) by EnSR assimilation with SOO. **d**, Mass loadings (ensemble mean) by EnSR assimilation without SOO, i.e., the operator  $H_k$  in Eq. (A5) does not select the grid cell in  $x(k)$ , but integrates all the vertical grid cells to calculate 2D mass loadings.

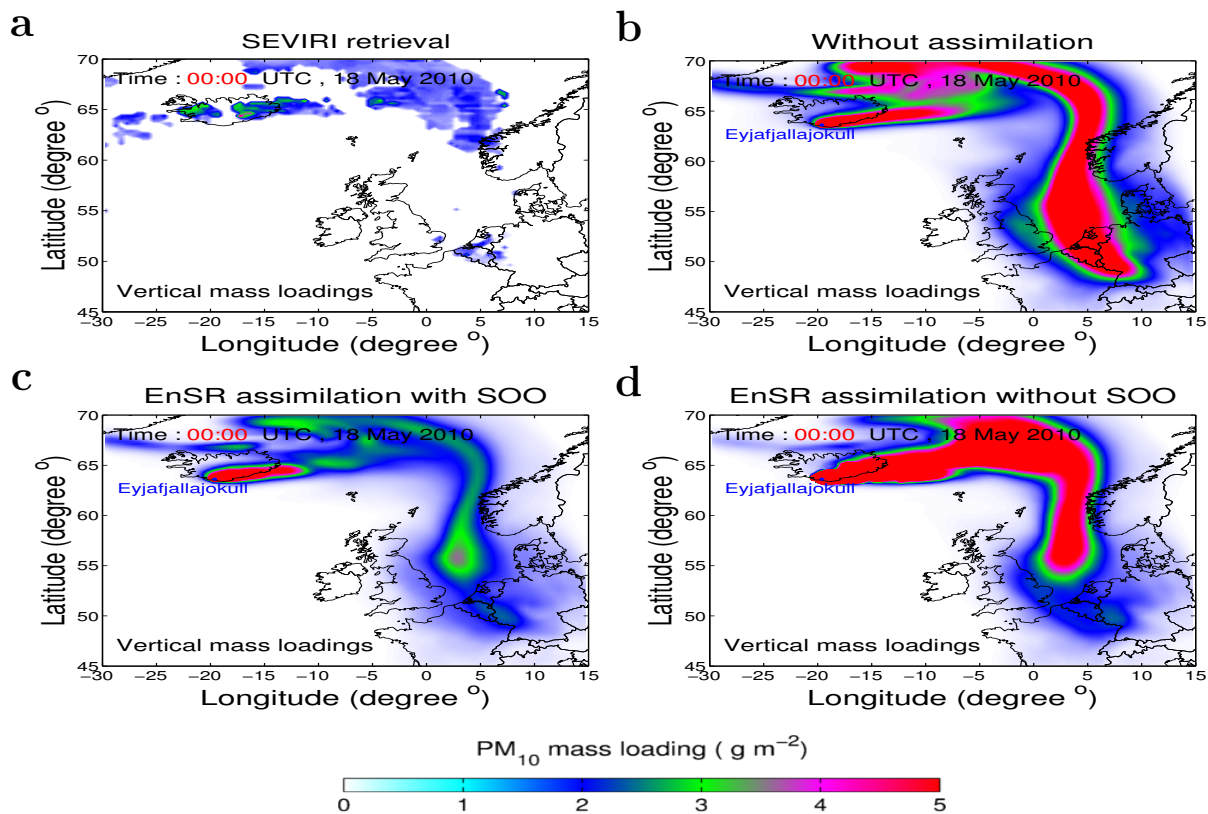


**Figure 6.**  $PM_{10}$  mass loadings with EnSR against the SEVIRI retrieval at 00:00 UTC 18 May 2010. **a**, SEVIRI retrieved mass loadings in the vertical direction, i.e.,  $M_V$  in Eq. (1). **b**, Simulated mass loadings without assimilation. **c**, Mass loadings (ensemble mean) by EnSR assimilation with SOO. **d**, Mass loadings (ensemble mean) by EnSR assimilation without SOO.

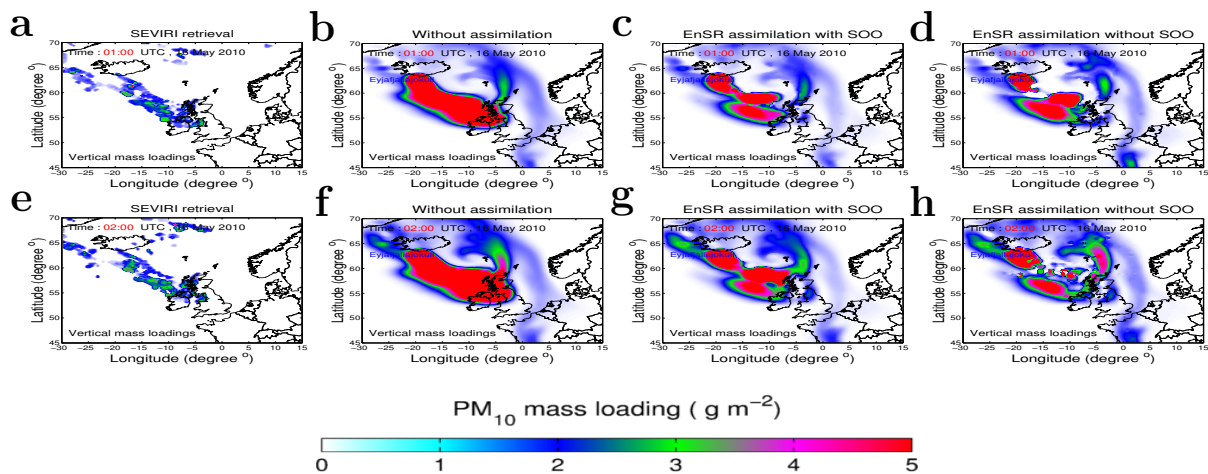


**Figure 7.** Evaluation of the assimilation effects by EnSR with SOO and without SOO at 01:00/0200 UTC 16 May 2010.

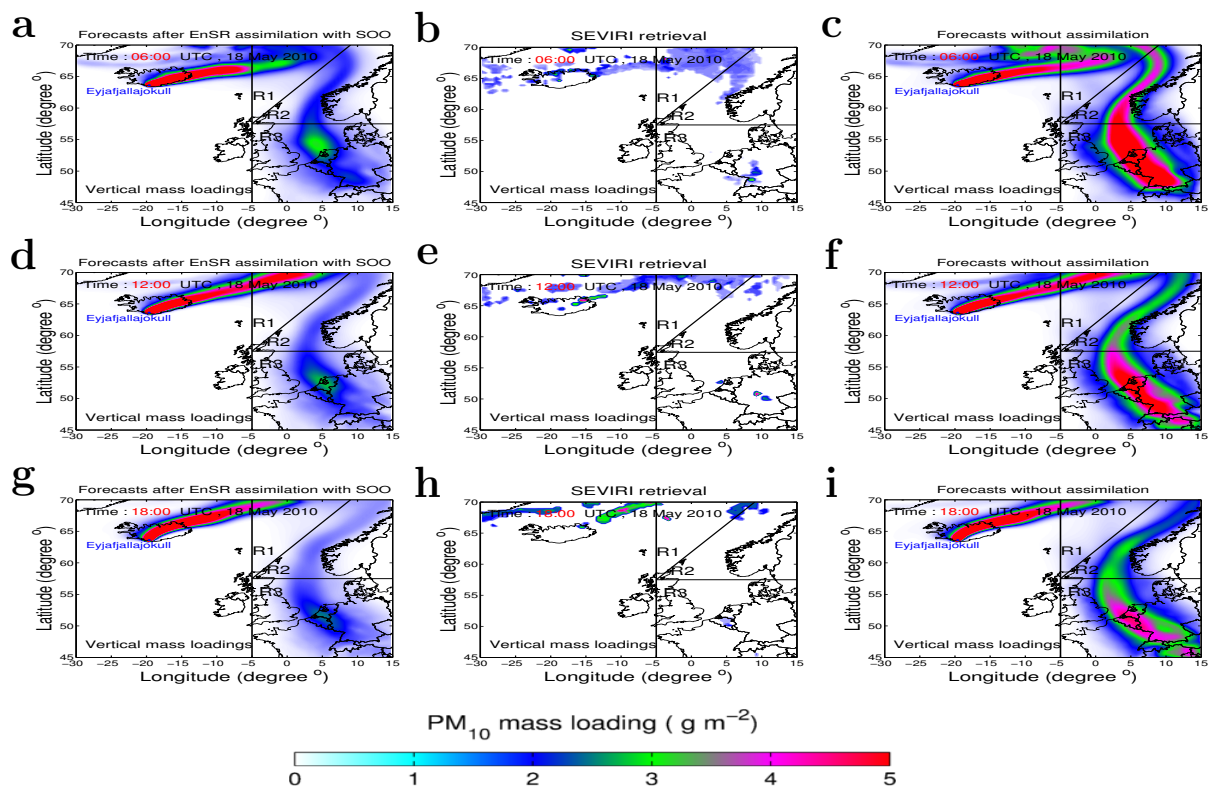


**Figure 8.** Evaluation of effective assimilation forecasts using satellite retrieved mass loadings (Date: 18 May 2010). R1–R3 represent the three distal regions to be evaluated with respect to the forecast after data assimilation.

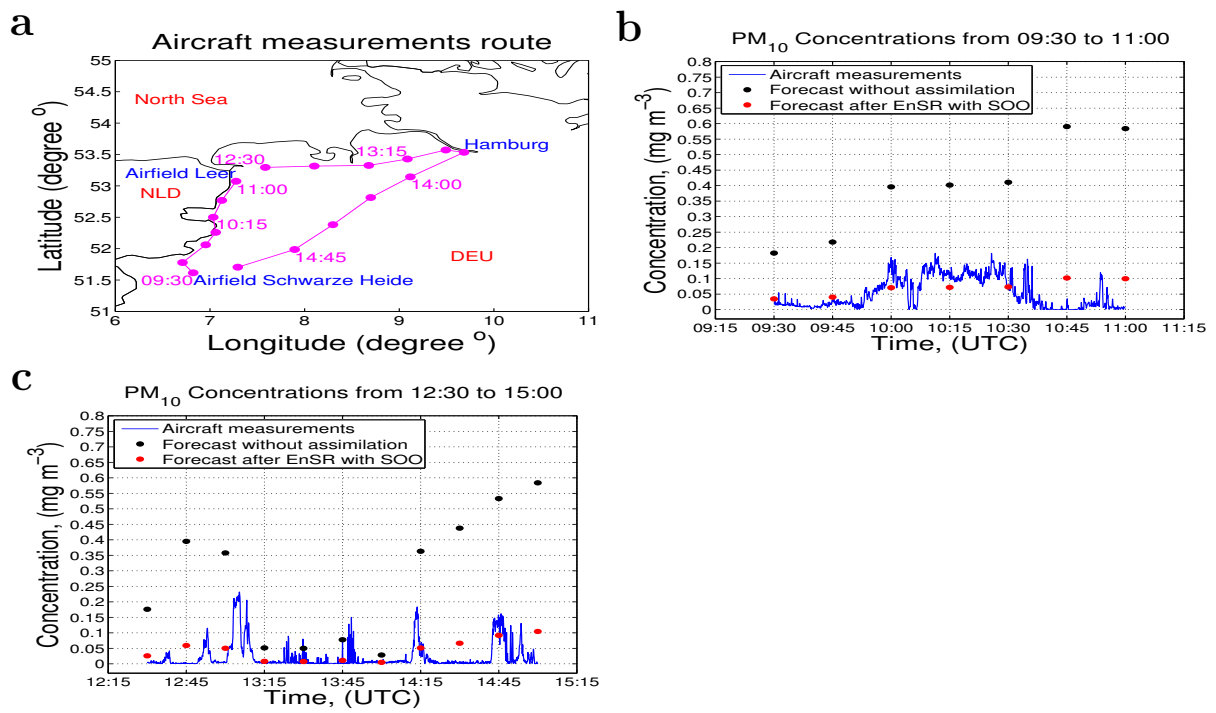


**Figure 9. Evaluation of effective assimilation forecasts using aircraft measurements (Date: 18 May 2010).** a, Aircraft measurements route. b, Comparisons of measurements, forecasts after assimilation (ensemble mean) or without assimilation from 09:30 to 11:00 UTC. c, Comparisons from 12:30 to 15:00 UTC.